ALASKA SEA GRANT PROGRAM

TECHNIQUES FOR MEASURING STRESS IN SEA ICE

by

Richard D. Nelson
Michael Tauriainen
and
James Borghorst

University of Alaska

Sea Grant Report No. 77-1
January 1977

ALASKA SEA GRANT PROGRAM

UNIVERSITY OF ALASKA

FAIRBANKS, ALASKA 99701

TECHNIQUES FOR MEASURING STRESS IN SEA ICE

Richard D. Nelson
Michael Tauriainen
and
James Borghorst

Alaska Sea Grant Report No. 77-1
January 1977

Contents

List of Figures

List of Tables

ABSTRACT

This report describes two techniques for measuring stress *in situ* in sea ice sheets. A technique using embedded load cells has been found successful in measuring compressive creep or failure stresses as well as moderate tensile stresses. A stress relief technique has been investigated and found unsuccessful. Design details are presented on transducers for each technique and cold-hardy instrumentation is discussed. A technique using inflated air bags to produce known stress fields is presented.

ACKNOWLEDGEMENT

The authors would like to thank Dr. Tunis Wentink, Jr., of the University of Alaska for his enthusiasm and encouragement during the project. We also thank Allyn Yoakum who helped in the laboratory and Helen Nelson who helped with the data reduction.

The research described in this report was carried out at the University of Alaska, Institute of Arctic Environmental Engineering during 1972.

This publication is the result of research sponsored by the Alaska Sea Grant Program, cooperatively supported by NOAA Office of Sea Grant, Department of Commerce, under Grant 04-5-159-35, and by the University of Alaska with funds appropriated by the State of Alaska.

I. INTRODUCTION

The development of the coastal resources of northern Alaska, particularly the oil, gas and mineral reserves, is impeded by the presence of sea ice during most of the year. Not only does sea ice present a static obstacle to shipping, but it also presents a dynamic hazard to fixed structures when wind, water, tidal forces and moving pack ice stress both the structure and the surrounding ice. In order to create marine facilities which make possible these developments, the design engineer must have available a knowledge of the forces, movements, and properties of the sea ice. The minimum data necessary for design of both off-shore and coastal structures are:

1. Failure strength of ice, *in situ*, when subjected to uniaxial and biaxial loads at naturally occurring rates.
2. The stress history of a typical ice sheet, its effect on ice properties, and its relations to the loading variables, particularly with respect to boundary conditions at the land-fast/pack ice border.
3. A knowledge of the interaction modes of rigid structures and stressed ice sheets.
4. A synoptic overview of ice deformations and properties in the region surrounding the structure site.

Present knowledge of these factors is insufficient for accurate, economical design.

While controlled laboratory tests can provide some information, field measurement of stresses as they occur in sea ice sheets appears to be the most expedient method of obtaining much of this data. However, until the present, techniques for measuring stress in sea ice have not been available, although Tabata and Ono [1972] and Frederking [1972] have done pertinent work. Therefore, this work was undertaken to develop techniques for in situ stress measurement in sea ice and to develop cold-hardy instrumentation for use with these techniques.

Workers in the fields of applied mechanics, geology, and rocket technology have used three basic techniques for experimental analysis of stress: Strain measurement (Hetenyi, 1950), stress relief (ibid.), and embedded force transducers (San Miguel and Duran, 1970). The most widely used of these is strain measurement via electrical resistance gages or mechanical dial gages; the attendant stress is calculated with the aid of the classical laws of elasticity. This works well so long as the gages are placed when the specimen is unstressed and the specimen is made of a linearly elastic material. For sea ice in situ neither of these conditions would be met, as the initial stress is unknown, and the material is highly inelastic. Given the variability of "elastic modulus" data, and the rapidity with which creep can occur in sea ice, even the assumption of quasi-elastic behavior is suspect unless one can measure "elastic" parameters for each installation and minimize the creep effects. Indeed, a much more detailed knowledge of the rheology of sea ice including time and stress history dependence would have to be available before strain measurement alone would form a useful basis for stress analysis.

Stress relief techniques are useful when the initial stress state is unknown and the material is elastic. Typical is the "hole boring" technique for plane stress developed by Mather [1934]. Three or more strain gages are placed in a circle on the stressed specimen. Boring a small hole at the center of the circle removes load bearing material, and results in a redistribution of stress which is sensed by the strain gages. The theory of elasticity allows calculation of the original stress tensor components from the changes in the three strain gage readings. Both tensile and compressive stresses can be analyzed. Although it cannot provide continuous stress data, a stress relief technique would be useful for sea ice to provide instantaneous pictures of stress. It overcomes the problem of unknown initial stress but is still subject to the question of rheology. However, since the hole is drilled rapidly, if appropriate short term "elastic" properties can be obtained, useful results may be possible. Thus, the hole drilling technique was chosen for development in this study.

An attractive possibility for materials which can be cast at moderate temperatures is the embedment of a stress transducer. If such a transducer can be constructed and accurately calibrated, a continuous record of stress during dynamic loadings is possible. A major theoretical problem is the interaction between the matrix and the included transducer. The theory of elasticity can handle only a limited number of simple cases so calibration of each host/transducer pair is required. If the elastic properties of the host are unknown or variable, considerable difficulty can be encountered in interpreting results. Fortunately, the theory of elasticity shows that the state of stress (stress concentration) in simple inclusions is relatively independent of the elastic properties of the matrix if the inclusion is much stiffer than the surrounding material (Muskhelishvili, 1953). Thus, one technique has been to cement glass cylinders in holes drilled in less stiff rocks and analyze stress in the rock matrix using the photo-elastic behavior of the glass (Jaeger and Cook, 1969). That is, the glass cylinder is used as a "stress transducer". Similarly, a miniature, cylindrical, uniaxial load cell using a piezo-resistance element has been used for short term (elastic) stress measurement in low modulus cast polyurethane and in solid rocket propellant by San Miguel and Duran [1970].

It is important that since the state of stress in a stiff inclusion is relatively independent of the host's properties, the stress in the inclusion will change only slightly if the host's properties change. If one views creep as continued "softening" of a material, one concludes that stiff transducers can be used in soft, creeping hosts to measure stress. Berry and Fairhurst [1966] have used Laplace transformes to confirm this for the cylindrical stress gage embedded in continuously creeping materials subject to non-reversing biaxial stress, and Hawkes [1969] has used glass cylinders to measure compressive stress in frozen soils. The use of elastic inclusions in creeping materials is elaborated later and forms the basis for the second method of stress measurement developed in this study.

The techniques previously used for ice all employ embedded transducers. Tabata and Ono [1972] have used resistance strain gages glued to a lucite bar as a transducer. They have also used a load measuring cell placed with pre-compression in a trench in the ice surface. The load cell was not totally embedded, but was covered with plastic foam insulation for weather protection. A third method investigated was the use of a soil pressure gage, commonly used in soil mechanics. Frederking [1972] has used a ring with resistance strain gages bonded to its surface and embedded in the ice to obtain the components of the stress tensor in plane stress. Richardson [1972] used a system of invar bars and dial gages, apparently to measure strain. These techniques are discussed in Section IV.

It would be well to outline here some of the unique properties of sea ice which complicate the matter of _in situ_ stress measurement.

1) Except for the top layer (10 inches or less) the crystals in sea ice have their c-axes randomly oriented in the horizontal plane. Thus, large sheets of sea ice can be expected to be isotropic in the plane of the sheet, but anisotropic in three dimensions.

2) The crystals in sea ice are typically columnar, of jagged cross section, density $4/cm^2$ or less in the plane of the sheet.

3) The crystals have a substructure of ice platelets and brine inclusions.

4) Sea ice creeps under stress.

5) The coefficient of thermal expansion may be either positive or negative, depending on ice temperature and salinity (Malmgren, 1927).

6) The rheological properties of sea ice depend on strain rate, temperature, age of the ice (brine content), and past stress history. However, the exact nature of these dependencies is only partially understood. Thus, the "elastic modulus" for sea ice has been given at values ranging from 2×10^5 psi to 1×10^6 psi, (Weeks and Assur, 1968), depending upon the prevailing conditions and method by which it is determined.

In addition to these factors, stress measurement is complicated by the fact that it must be done in the field. Thus, a transducer system which would be used to evaluate stress history must be capable of reliable long term calibration, unaffected by weather or salt brine, and free from zero drift due to temperature, age, corrosion, or ice creep. The requirements are less exacting for a stress relief system, since it measures dynamic strains over only a few minutes. However, a stress relief system must be capable of being deployed rapidly to maximize the amount of data gathered in a day. Each method should be capable of in situ calibration with known stresses, if possible.

At the start of this project, several major problem areas were identified. Of particular concern was creep of the ice and the attendant changes of reading for buried transducers. In spite of the encouraging results of Berry and Fairhurst and of Hawkes, it was felt that the unknown interaction of a transducer with either the platelet structure or the polycrystalline structure of sea ice might complicate matters. In addition, ice is known to crack extensively at failure and perhaps during creep (see Sprenger, 1972 for discussion), the cohesion of ice and metals can be weak, and Richardson [1972] has described salt migration to stress concentrations at transducers. In short, it was unknown whether continuum behavior could be expected of sea ice for either a buried transducer or stress relief technique. In addition, there was a question whether the sensitivity of either technique would be linear or even reproducible over a full range of stress up to both tensile and compressive failure. For transducer methods, the relation of low and high frequency response was of concern. Finally, it was anticipated that standard electronic equipment might operate poorly in cold environments and that a certain amount of equipment development might be needed.

The following report describes the special equipment developed and the results of studies on both transducer and hole drilling techniques of stress measurement.

II. EQUIPMENT

A. Ice Specimens

Most of this work was done in temperature controlled cold rooms, using ice grown in the laboratory from tap water doped with sodium chloride to 30-35 p.p.t. salinity. The ice was grown in large tanks with open tops and insulated sides and bottoms so as to simulate the uniaxial growth of normal sea ice. Dykins [1966] has shown that ice grown in this way from sea water is similar to normal young sea ice until about half of the container is frozen. Concentration of the excluded brine beyond this point makes the ice less and less like true sea ice. The cold rooms in which the ice was grown were held at -10° to $-15^{\circ}C$. In order to obtain a fine grain structure, the initial skim ice which formed in a tank was crushed into fine particles. The containers used here were over two feet deep, and the top 12 inches was used for specimens. Where it was necessary to obtain a deeper sample which did not include a transition layer, the water in a container was diluted daily to maintain 30-45 p.p.t. salinity; brine was drained off at the same rate as fresh water was added to avoid disturbing the skeletal structure at the water-ice interface. One container was an integral ice growing tank and compression testing machine of 12 inch depth. Daily brine dilution allowed ice in this tank to be frozen all the way to the bottom.

B. Electronic Equipment

As anticipated, obtaining satisfactory recording equipment has proved to be somewhat of a problem. D.C. powered resistance strain gage transducers were used throughout this work and because of design limitations their signal was always less than 1 millivolt. The first instrument used to record these signals was a Leeds and Northrup multi-channel Speedo-max H recorder with a range of 1 m.v. full scale. A Zeltex 133-03 operational amplifier was used as an impedence buffer between the recorder amplifier and the recorder's switching relays. Data points were recorded at one per second. The power used by this instrument is sufficient to keep its electronic components warm at -20^{O}C, but the switching relays are exposed and extra heat was required to keep them from sticking. Even with this, the relays are noisy at cold temperatures, resulting in a poor trace. The amplifier of the L and N recorder is slightly temperature sensitive, so its front door must be left continually shut. This recorder has performed adequately in the cold room, which has a dehumidification coil to remove moisture from the air. However, it did not perform well in a June, 1972, field test at Barrow. Either due to air transportation, "dirty" A.C. power from a portable generator, or excessive exposure to humid air, trouble developed in the main amplifier after several hours use on the sea ice. A second unit suffered similarly. These units continue to be used in the laboratory, but not field work.

A Honeywell portable (D.C. power) light beam oscillograph has also been used in the laboratory. It uses enough power to remain at 25^{O}F when placed in a ventilated protective box with the cold room at -20^{O}C. No particular problems have developed in the laboratory, other than those inherent in this type of recorder. In the field, power consumption would be a problem, as it uses up to 200 watts and requires frequent paper changes. It was conceived as a recording medium for sites where power was available or visits could be made every few days. Its multi-channel, high speed capabilities make it perfect for use during periods of intense ice activity.

For long term unattended recording, Rustrak four channel recorders, Model 388, have been used with success. These recorders have a sensitivity of $\pm$10 millivolts full scale, use only 0.1 watt at 12 volts, and record a series of dots on pressure sensitive paper. With 16 seconds between dots, and one inch per hour chart speed, these recorders are useful for recording stress variations occuring over ten minutes or more. They provide a compact, rugged, relatively cheap recording package with accuracy of five percent. A disadvantage is that a switching relay is used to provide the multi-channel capability.

Several manufacturers of tape recorders, graphic recorders, and electronic equipment were contacted concerning the low temperature capability of their products. In most cases, they were unwilling to specify their products to temperatures lower than freezing. The possible mechanical problems which were cited were stiffening of rubber drive rollers in tape and paper transports, lubrication, and brittleness of paper at cold temperatures. Two electronic problems are the change of transistor parameters with temperature, and the freezing of electrolytic capacitors (Sackinger, 1972), although we have used electrolytic capacitors for inactive filters at $-20^{\circ}C$ with no apparent problems. The manufacturers of operational amplifiers routinely specify their units to $-20^{\circ}C$ and will select units suitable for lower temperature on request. These amplifiers have been very useful, particularly the Analog Devices Model 153 which requires extremely low power. In all cases, input offset current and voltage are present and temperature sensitivity can be extreme. However, the proper choice of device and circuitry minimize these problems. A resistance bridge with one leg shunted by a thermister has been used to counter temperature induced zero drift.

C. Stress Transducers

The load cells used as stress transducers all employ bonded resistance strain gages to provide an electrical signal proportional to the applied load. In order to increase their sensitivity, most commercially available load cells employ beams or plates in bending as the strain-gaged element. Such a transducer is indeed sensitive, but is also quite flexible. As discussed elsewhere in this paper, a transducer for sea ice must be several times stiffer than the ice surrounding it, which may have an elastic modulus as high as 1×10^6 psi. In order to meet this criterion, we have found it necessary to use simple tension links rather than bending elements in transducers.

Consider a right circular cylinder of diameter D, length L, with a reduced cross section of diameter d, length l, as shown in Figure 1. Strain gages will be applied to the reduced section to measure the load F, applied at the ends. The stress in the reduced area, σ_r, is

$$\sigma_r = \frac{F}{\frac{\pi d^2}{4}} = \frac{4}{\pi} \frac{F}{d^2} \tag{1}$$

and the total change of length of the bar is

$$\Delta L = \Delta \ell + \Delta(L-\ell)$$

$$\Delta L = \frac{\sigma_r}{E_t} \ell + \frac{\sigma}{E_t} (L-\ell) \tag{2}$$

$$\Delta L = \frac{1}{E_t} \left[\left(\frac{4}{\pi} \frac{F \ell}{d^2} \right) + \frac{4F}{\pi D^2} (L-\ell) \right]$$

$$\Delta L = \frac{4F}{\pi E_t} \frac{L}{D^2} \left(1 + \frac{D^2}{d^2} \frac{\ell}{L} - \frac{\ell}{L} \right) \tag{3}$$

E_t is the elastic modulus of the transducer material, and σ is the stress in the unreduced section.

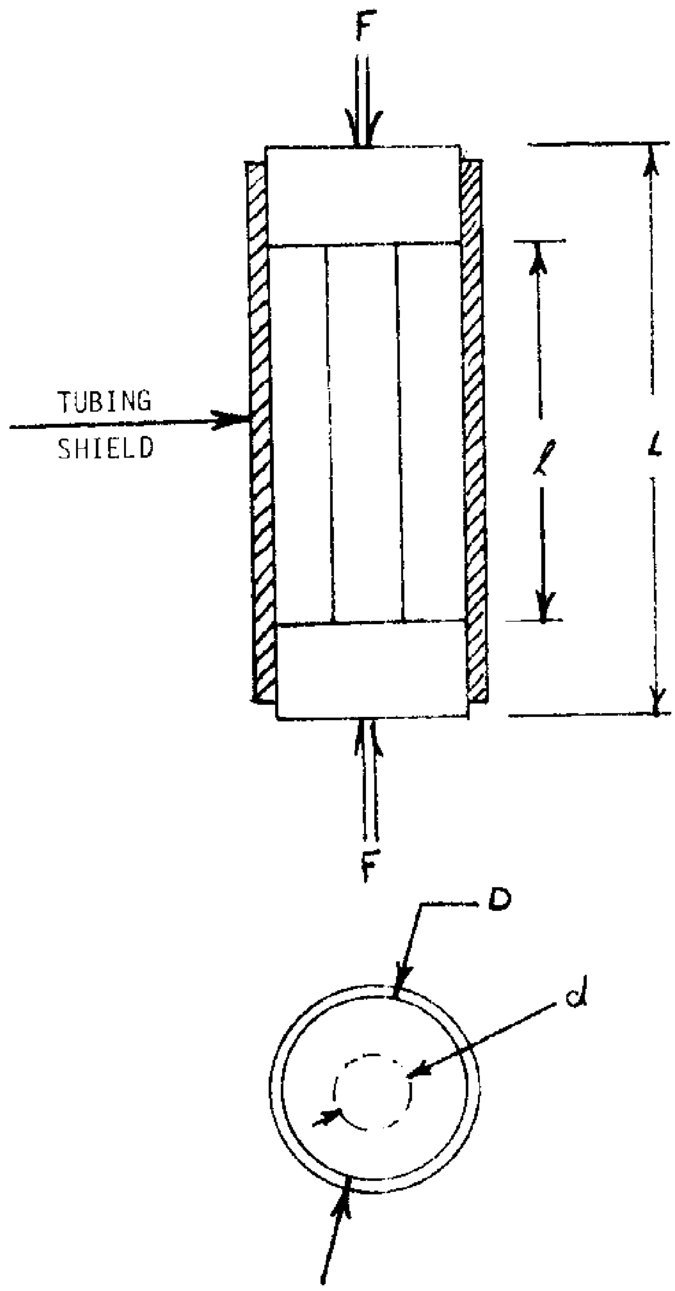

FIGURE 1. Stress transducer geometry.

The spring constant for the transducer is

$$K_T = \frac{F}{\Delta L} = \frac{\pi}{4} E_T \left[\frac{1}{\frac{L}{D^2} + \frac{\ell}{d^2} - \frac{\ell}{D^2}} \right];$$

The spring constant for an equal volume of ice would be

$$K_i = \frac{F}{\Delta L} = \frac{E_i A_i}{L} = \frac{K\pi D^2}{4L} E_i$$

Then the ratio of the transducer stiffness to ice stiffness is

$$\frac{K_t}{K_i} = \frac{E_T}{E_i} \left[\frac{1}{1 + \frac{\ell D^2}{L d^2} - \frac{\ell}{L}} \right]$$

As shown in section IV, this ratio must be larger than one and preferably larger than five for a successful stress transducer. The three most likely choices for transducer material are:

Stainless Steel	-	$E_t/E_i = 30$
Brass	-	$E_t/E_i = 15$
Aluminum	-	$E_t/E_i = 10$

with Young's Modulus for ice taken as 1×10^6 psi. It is easy to see that the stiffest transducer will use stainless steel and minimize the length of the reduced section while maximizing its diameter. However, several other factors enter into the design of these transducers. First, the range of stresses encountered in sea ice is 10 to 500 psi, which is in the lower portion of the range normally measured by the strain gages which would be used as sensing elements. Two design alternatives are possible to increase the signal from such a transducer: first, use a low modulus material such as aluminum; second, use a much reduced diameter for the gaged section. If these alternatives do not provide adequate signal, either high gage-factor strain gages or high gain amplifiers must be used. A second restriction is the uniformity of stress in the reduced section: St. Venant's principal implies that the length of the reduced section must be several times its diameter if strain gages placed at the halfway point are to measure the average stress applied to the transducer face. Third, it is desirable to use a four-arm bridge because of its inherent temperature compensation. Finally, the diameter of the upper and lower faces of the transducer should be large in comparison with typical ice crystal size but small in comparison with the size of the specimen in which it is embedded.

Figure 2 shows a stress transducer which was designed according to the above criteria. A 1 inch diameter aluminum cylinder, 3 inches long, has a 2 inch long by 1/2 inch diameter reduced section. Four strain gages parallel and perpendicular to the axis of the cylinder are connected in a bridge to read tension or compression in the bar and provide inherent temperature compensation. The aluminum cylinder fits inside a copper tube and has 1/2 inch diameter steel bolts on each end to provide a grip for tensile stresses. The strain gages were coated with GageKote 2 sold by Bean and Company and with silicone rubber. The copper tube was sealed to the aluminum bar with silicone rubber and the entire assembly coated with GageKote 2. Lead-in wires were sealed into a hole in the aluminum bar with silicone rubber.

The transducer in Figure 2 has a long, narrow geometry. To investigate the effects of geometry on performance, a short, broad transducer was designed. A shorter version of Figure 2, 3 inch diameter by 1 inch long was tried but was unsatisfactory because the load carrying member was too short to average out non-uniformly applied loads. Figure 3 shows a more successful short transducer. Four 1/2 inch square stainless steel bars, 1 inch long, carry the load between two 3 inch diameter by 1/2 inch thick aluminum plattens. Each bar has one axial strain gage and one transverse strain gage, and all gages

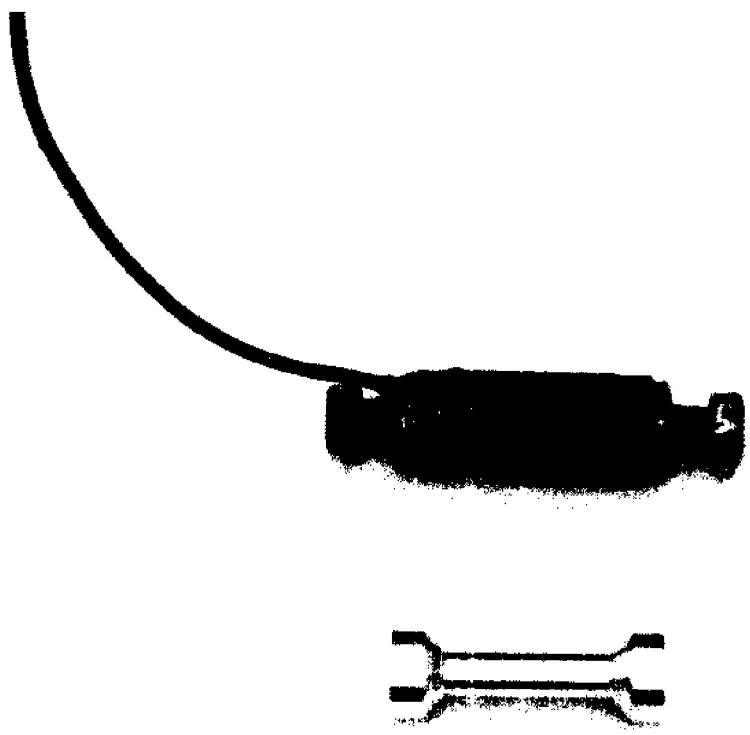

FIGURE 2. Stress transducer used for tests. Strain gages were fixed to the 3 inch long blank shown. Above the blank is a finished transducer with steel end-bolts and a copper protective sleeve.

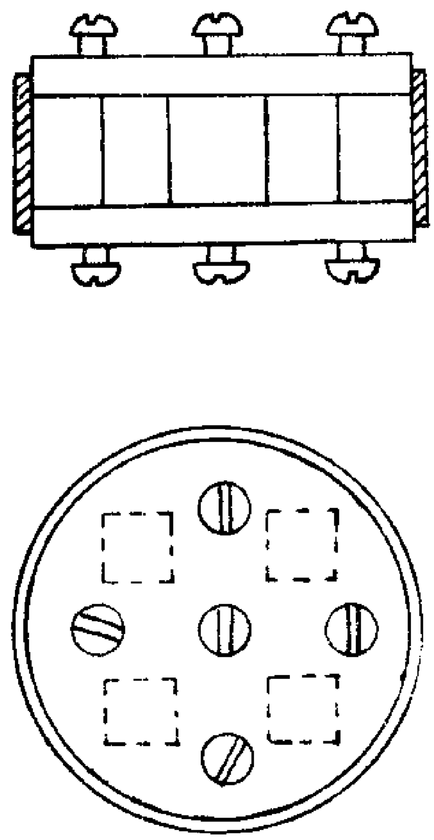

FIGURE 3. Flat transducer.

are connected to form a 4-arm bridge. Bolts in each platten provide gripping surfaces for the ice. Again, a copper sleeve and appropriate sealing compounds are used.

We have mentioned the use of the 4-arm bridge to provide inherent compensation for temperature induced strains. In addition, one may select strain gages which are themselves temperature compensated for use with steel, aluminum, etc. Normally these gages are compensated only near room temperature. For use at lower temperatures, better results are obtained if the strain gages are selected as if the transducer material had a somewhat higher coefficient of thermal expansion. For instance, we have used gages designed for 15 p.p.m. per ^{0}F.

D. Displacement Transducers

For stress relief studies it was necessary to have transducers which would measure displacement between two gage points. Again bonded resistance strain gages were used to provide electrical read out. The gages were applied to 0.030 inch thick aluminum leafs which were the flexible elements in the transducer shown in Figure 4. The 1/4 inch diameter by 1/2 inch long gage points are embedded at the surface of the ice under test; strain in the ice causes flexing of the aluminum leaves which is read out by the strain gages. In order to register strain in the ice, a force must exist at each gage point; this fact limits the sensitivity of such a transducer because the gage points tend to creep back into the ice. Because these transducers were to sense small elastic motions during stress relief, it was arbitrarily decided that the nominal stress at the gage points (force divided by project area) should be no more than 1/10 the stress in the ice, assuming elastic deflections. The transducers were designed for use with one inch gage lengths, use two 1.25 by 0.25 by 0.030 inch aluminum leaves in parallel with both ends

FIGURE 4. Strain measuring transducer. The right hand leg is the flexible element and consists of two short aluminum flexible leaves which are clamped to the 1/2 inch square top bar and to the 1/2 x 1/8 inch lower plate which is embedded in the ice. Silicone rubber is used as a water proofing agent and leads to the massive appearance.

clamped, and have a sensitivity of 0.2 μ v./v. per micro-inch of displacement. When used on a 3 inch gage length, the stress at the gage points is 0.32 times the stress in the ice, assuming a modulus of elasticity of 5×10^6 psi for the ice.

E. Air bags

The hole-drilling procedure required that a means be developed for applying a known pressure on the inside or outside of tubular specimens of ice. The low required pressure (10-50 psi) suggested the use of inflated air bags such as doctors use to measure blood pressure. Figure 5 shows an air bag which is used to provide internal pressure on an 8 inch diameter hole. A steel core and plywood headers provide sealing and support for a cylindrical rubber membrane cut from an automobile inner tube. A pressure of 2 psi is enough to distend the membrane well beyond 9 inches diameter. The headers should provide a snug fit in the hole to prevent the membrane from bulging out the top.

An air bag used to provide pressure on the outside of a 16 inch diameter cylinder is shown in Figure 6. It is constructed from plastic coated nylon and cemented to a sheet steel backing plate. In use, it is inserted in a circular trench cut in the ice. The bag should be inserted at least one inch below the ice surface to prevent bulging. The nylon, while strong enough to resist tearing at 40 psi, does develop serious leaks where the plastic coating blows out between threads. A better material might be a rubberized canvas, or a nylon shell and inner rubber membrane. An all rubber bag could be used if adequate assembly techniques are available, and if headers are provided to limit bulging at top and bottom.

A flat air bag, similar to the mining engineer's flat-jack, was incorporated into the integral ice tank and compression tester shown in

FIGURE 5. Air bag used to provide internal pressure on hole.

FIGURE 6. Air bag used to provide external pressure on cylinder.

Figure 7. An insulated steel frame supports a plywood tank, 32 inch by 38 inch by 14 inch deep. One wall of the tank is fitted with the flat air bag. After ice is frozen in the tank and the sides have been relieved with a chain saw, uniaxial compression can be applied by inflating the bag.

III. HOLE DRILLING METHOD

A. Theory

The hole drilling method relies on the theory of elasticity to predict the stress distribution and deformation around a hole in a loaded body. For instance, consider a large plate under uniaxial stress, σ. If a hole is bored in the plate, while it is loaded, a redistribution of stress occurs in the region of the hole so that the stress is given in polar coordinates by (Sokolnikoff, 1956):

$$\begin{aligned} \sigma_r &= \frac{\sigma}{2}\left[\left(1-\frac{R^2}{r^2}\right) + \left(1-\frac{4R^2}{r^2}+\frac{3R^4}{r^4}\right)\cos 2\theta\right] \\ \sigma_\theta &= \frac{\sigma}{2}\left[\left(1+\frac{R^2}{r^2}\right) - \left(1+\frac{3R^4}{r^4}\right)\cos 2\theta\right] \qquad (6) \\ \tau_{r\theta} &= -\frac{\sigma}{2}\left(1+\frac{2R^2}{r^2}-\frac{3R^4}{r^4}\right)\sin 2\theta \end{aligned}$$

where R = hole radius, r = radial distance to point of interest, and θ = angular coordinate to point of interest measured from stress axis. The stress "added" by boring the hole is the difference between the uniform stress and the value given in Equation (6):

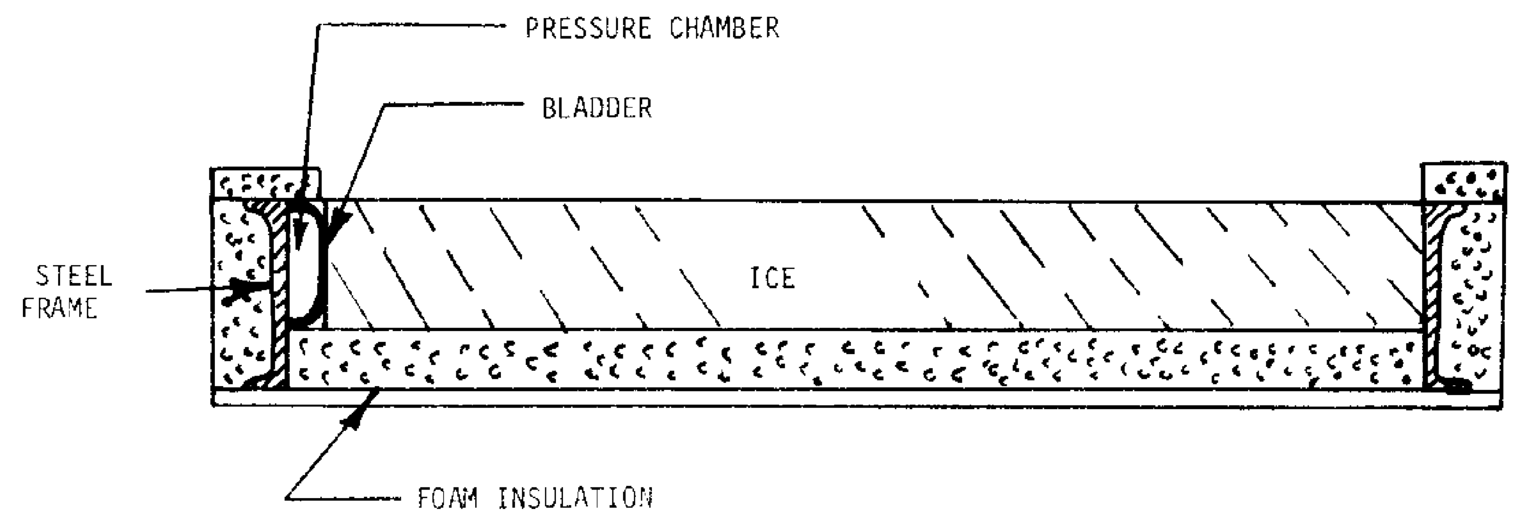

FIGURE 7. Integral ice growing tank and compression tester.

$$
\begin{aligned}
\sigma_{r\,\text{added}} &= \left(\frac{-R^2}{2r^2} + \frac{3R^4}{2r^4}\cos 2\theta - \frac{2R^2}{r^2}\cos 2\theta \right)\sigma \\
\sigma_{\theta\,\text{added}} &= \left(\frac{R^2}{2r^2} - \frac{3R^4}{2r^4}\cos 2\theta \right)\sigma \qquad (7) \\
\tau_{r\theta\,\text{added}} &= \left(\frac{R^2}{r^2} - \frac{3R^4}{2r^4} \right)(\sin 2\theta)\,\sigma
\end{aligned}
$$

The strains resulting from boring the hole can be found from these stresses with the aid of Young's modulus and Poisson's ratio. If two principal stresses are present, two sets of stresses as in (7) may be superimposed.

In the usual case, the body will be stressed by unknown principal stresses 6m and σ_m, Figure 8. Either radial or tangential strains are measured at three points around the hole as it is drilled, and the principal stresses are calculated by reversing the process described above. If ϵ_0, ϵ_{45}, ϵ_{90} are tangential strains measured at 0^o, 45^o, to 90^o to one another, the principal stresses are (Riparbelli, 1950), (Milbradt, 1951):

$$
\sigma_{n,m} = E\left[-(1/2)\, \frac{\epsilon_0 + \epsilon_{90}}{(\nu+1) + \frac{1}{r_2-r_1}\int_{r_1}^{r_2} \left[\left(r+\frac{R^2}{r^2}\right) - \nu\left(1-\frac{R^2}{r^2}\right) \right] dr} \pm \frac{1}{\cos 2\theta}\, \frac{\epsilon_0 - \epsilon_{90}}{-(1+\nu) + \frac{1}{r_2-r_1}\int_{r_1}^{r_2} \left[\left(1+\frac{3R^4}{r^4}\right) + \nu\left(1+\frac{3R^4}{r^4} - \frac{4R^2}{r^2}\right) \right] dr} \right] \qquad (8)
$$

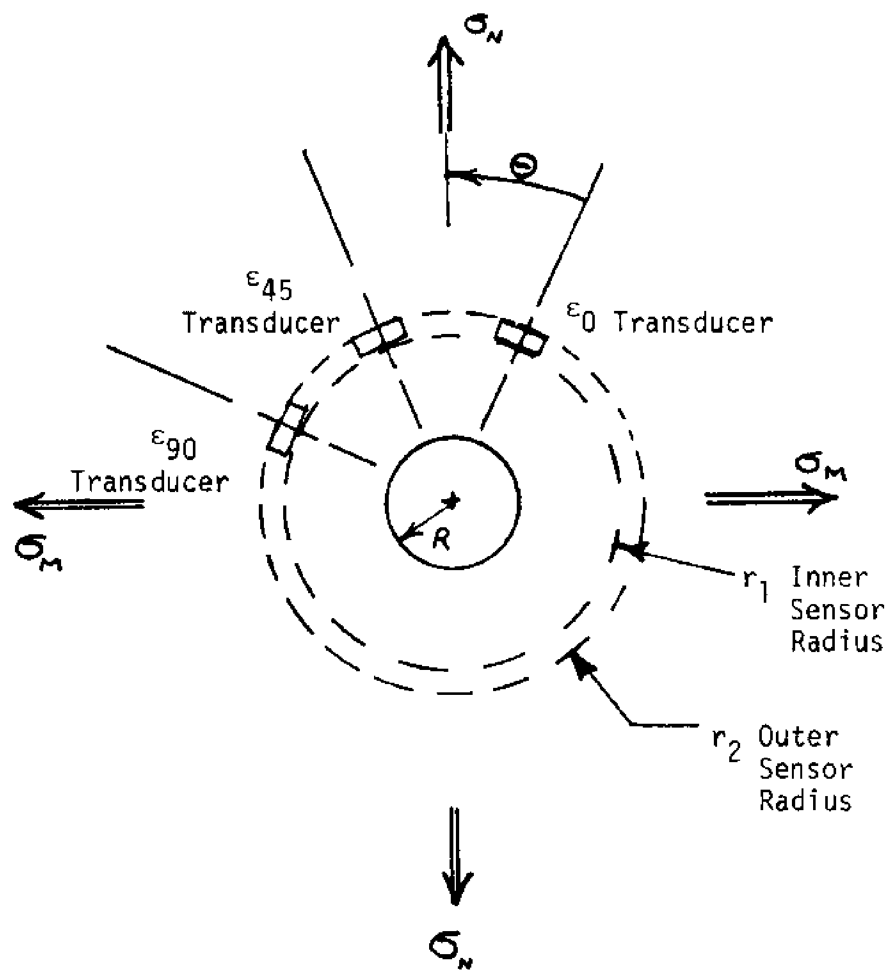

FIGURE 8. Location of strain sensors in a hole drilling analysis.

with E and ν being Young's modulus and Poisson's ratio. The integrals are taken between the inner and outer radii of the strain sensors. The location of the principal stresses is given by:

$$\tan 2\theta = \frac{2\varepsilon_{45} - \varepsilon_0 - \varepsilon_{90}}{\varepsilon_{90} - \varepsilon_0} \tag{9}$$

For sea ice, the stress at the top surface might be evaluated by measuring tangential strains about a hole drilled by a standard ice auger.

An important requirement for the use of this method is knowledge of the modulus of elasticity and Poisson's ratio for the ice being tested. In most cases, these quantities will be unknown and, given the variability of available data, must be determined by separate tests. It seems logical that best results will be obtained if these auxiliary tests are performed *in situ* using the same deflection or strain measuring devices as were used in the hole drilling process. The well known deformations of an internally or externally pressurized elastic cylinder provide a way to do this, since a hole is already present in the ice, and a trench may be cut surrounding it. The tangential strain will be (Timoshenko, 1956):

$$\varepsilon_T = \frac{1-\nu}{E}\,\frac{a^2P_i - b^2P_o}{b^2 - a^2} + \frac{1+\nu}{E}\,\frac{a^2b^2(P_i - P_o)}{(b^2 - a^2)r^2} \tag{10}$$

where
- a = inner radius of cylinder
- b = sensor radius
- e = elastic modulus
- P_i = internal pressure
- P_o = external pressure
- r = sensor radius
- ν = Poisson's ratio

Data from two independent tests can be combined to yield both E and ν.

Because the equations are linear in pressure, measurements cannot be restricted to pressure on the hole alone. In this work, several combinations of internal and external pressure were used.

B. Hole Drilling Test

In order to test the method, several 10-inch cubes of salt ice were stressed at 50 psi uniaxial compression. One inch diameter holes were drilled with tangential deformations on a 2 inch circle measured as in Figure 8 with $\Theta = 0$ and $\sigma_m = 0$. The deflection measuring transducers described in Section II were used with 1 inch gage lengths, and a 1 inch diameter air bag was used to provide internal pressure of 20 psi to the hole. Consistent results were not obtained, either between tests, or within a given test. It was suspected that the small scale of the test was at fault since the size of the hole was not much larger than one or two grains of the ice, and the 1 inch gage length might contain only one or two grains. Thus, it was not surprising that a continuum analysis failed to describe the behavior of an agglomeration of several ice grains. In order to approach the realm where continuum behavior could be expected, full scale tests were designed using an 8 inch diameter hole, 12 inch diameter sensor circle, 2 inch gage lengths, and a 16 inch external trench. Tests were attempted at Barrow, Alaska in June 1972, but could not be completed because of instrument failures.

One test was completed in the cold room at Fairbanks using a 32 x 38 x 12 inch thick ice sheet under 20 psi compression at a temperature of -14°C. The displacement transducers described in II D, extended to measure over a 3 inch gage length, were frozen into the ice with fresh water at locations parallel to, perpendicular to, and 45° to the applied stress. The ice, which had been previously stressed, was loaded to 20 psi uniaxial compression for five minutes, unloaded for 10 minutes, and reloaded to 20 psi. After half an hour, an 8 inch hole was drilled through the stressed ice. Next an 8 inch diameter bladder was inserted in the hole and used to provide 20 psi internal pressure on the periphery of the hole. Three load and unload cycles were performed. Next the 20 psi uniaxial stress was released, applied, and released with no pressure on the hole. A trench was cut outside the sensors, isolating a cylinder of ice approximately 8 inch I.D. by 16 inch O.D. by 12 inch long. A flat air bag was curled around the cylinder and inserted in the trench to provide external pressure on the cylinder. Two cycles of 10 psi external pressure and release were performed. Next were two cycles of 10 psi external pressure, 10 psi internal pressure added to the external pressure, and releasing both pressures.

Table 1 summarizes the results of the hole boring tests in terms of micro-inches/inch strain registered by each transducer. Figure 9 shows the actual data taken during the hole drilling while Figure 10 shows the data obtained for the first internal pressure test. As seen in Figure 10, creep usually occurred following pressurization and recovery was present following pressure release. Therefore, the asymptotic approximations shown have been used to evaluate a quasi-elastic response. Table 2 shows the values of Young's modulus and Poisson's ratio calculated for each gage location for tests 1 through 9, using test 1 as a basis -- e.g., loading tests 1 and 4 were used to solve simultaneously two independent equations for E and ν obtained from equation 10, giving $E = 1.07 \times 10^6$ psi and $\nu = 1.69$.

C. Discussion of Hole Drilling

The calculated values of E and ν Table 2 show a surprising inconsistency both in magnitude and sign. Since an accurate knowledge of these

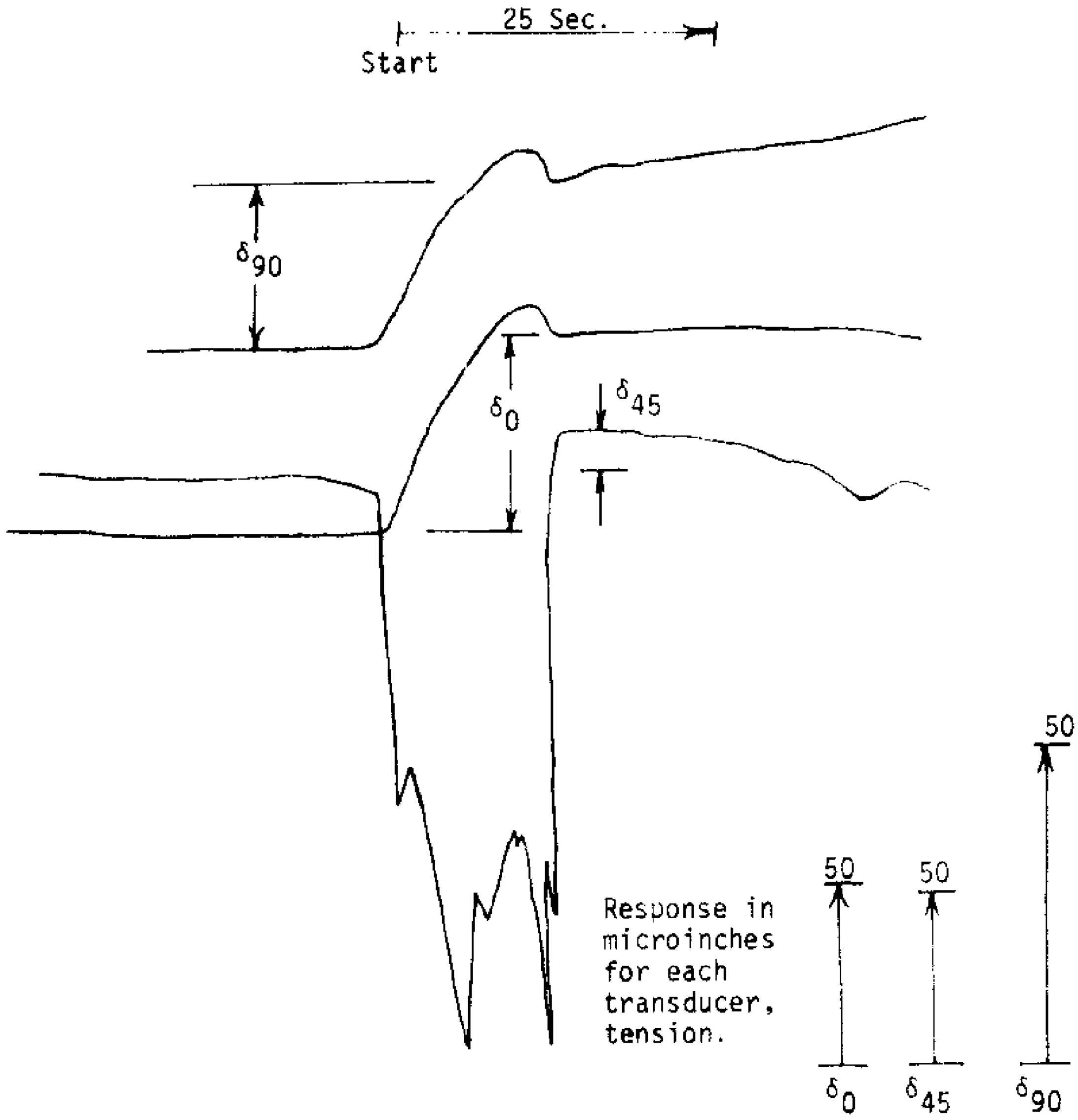

FIGURE 9. Strain transducer responses while drilling 8 inch hole in ice under 10 psi compression. Strain transducers oriented as in Figure 9 with $\theta = 0$.

TABLE 1

Strain Transducer Readings During Hole Boring.

Orientation	Change Microinches Per Inch	Tension or Compression
0°	17.4	T
45°	3.7	T
90°	9.2	T

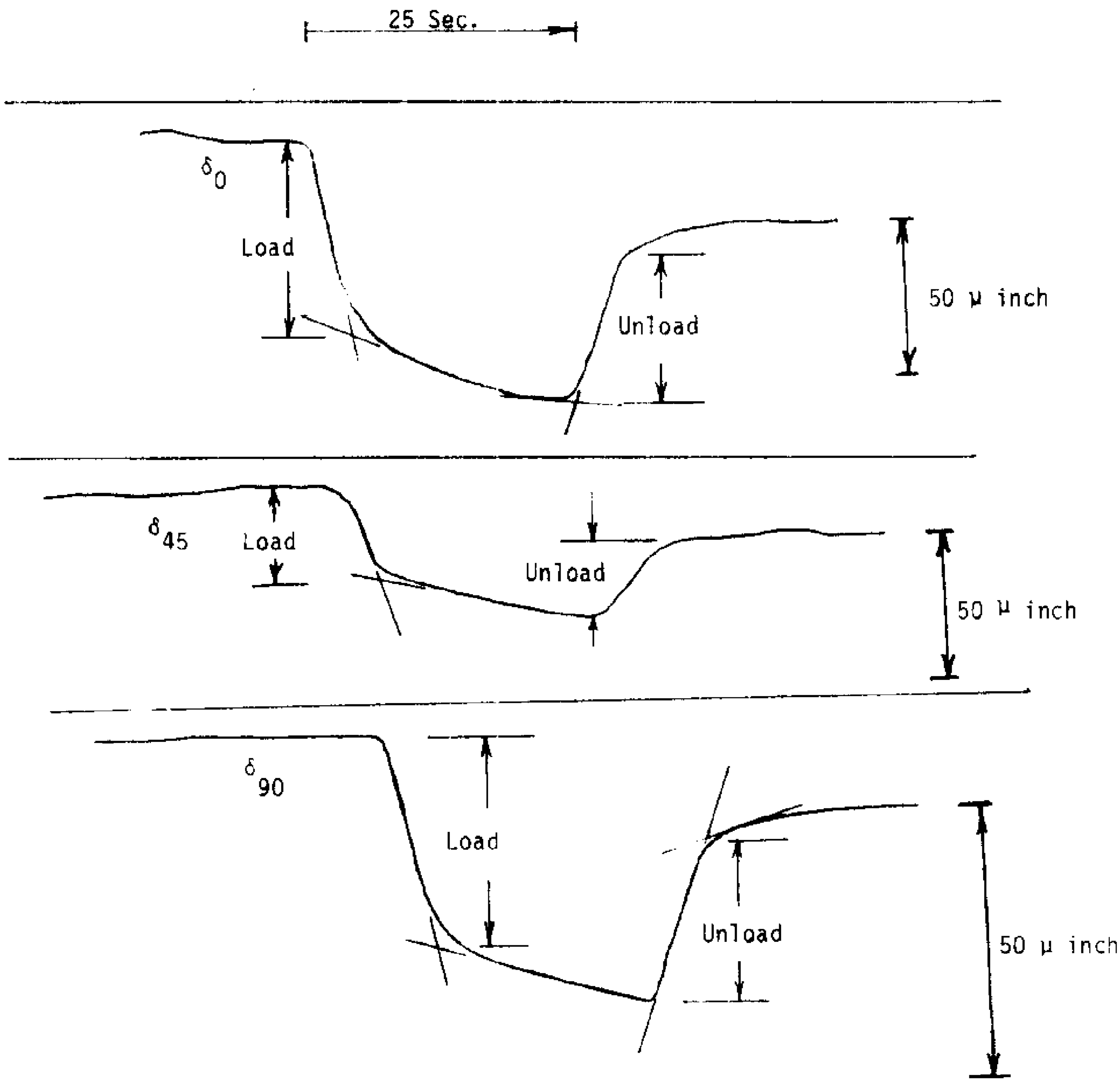

FIGURE 10. Strain transducer responses to 20 psi internal pressure on 8 inch hole in 32 x 38 inch block.

TABLE 2a. STRAIN DATA AND CALCULATED ELASTIC CONSTANTS.

All data for application of internal or external pressure on salt ice ring.

Test 1 taken as base test for calculations.
Tension taken as positive.

Test	$P_{int.}$ P.S.I.	$P_{ext.}$ P.S.I.	Strain Transducer Location	Measured Strain in/inx10^6	Elastic Modulus PSIx10^{-6}	Poisson's Ratio
1	20	0	0° 45° 90°	23.73 10.8 12.9		
2	20	0	0° 45° 90°	17.93 7.67 12.03		
3	20	0	0° 45° 90°	23.73 10.80 13.40		
4	0	10	0° 45° 90°	- 7.0 -16.93 - 9.53	1.07 1.09 1.39	1.69 0.190 0.841
5	0	10	0° 45° 90°	- 7.23 -21.6 -11.2	1.06 0.919 1.278	1.66 -0.0124 0.683
6	0	10	0° 45° 90°	-31.87 -21.9 -11.4	0.566 .911 1.267	0.265 -0.0233 0.665
7	10	10	0° 45° 90°	-22.66 -18.51 - 8.40	0.417 0.695 0.9537	-0.153 -0.286 0.199
8	0	10	0° 45° 90°	-29.00 -20.67 -10.7	0.598 .948 1.308	0.357 0.0228 0.727
9	10	10	0° 45° 90°	-24.93 -19.12 - 8.20	0.438 0.681 0.962	-0.093 -0.303 0.211

TABLE 2b. STRAIN DATA AND CALCULATED ELASTIC CONSTANTS.

All data for removal of all internal or external pressure on salt ice ring.

Test 1 taken as base test for calculations.
Tension taken as positive.

Test	$P_{int.}$ P.S.I.	$P_{ext.}$ P.S.I.	Strain Transducer Location	Measured Strain in/inx10^6	Elastic Modulus PSIx10^{-6}	Poisson's Ratio
1	20	0	0° 45° 90°	-15.1 - 8.6 - 9.67		
2	20	0	0° 45° 90°	-17.9 - 9.23 -10.33		
3	20	0	0° 45° 90°	-15.93 -10.47 -10.33		
4	0	10	0° 45° 90°	5.067 15.43 10.87	1.627 1.245 1.48	1.585 0.076 0.432
5	0	10	0° 45° 90°	8.13 24.67 14.4	1.394 0.883 1.25	1.168 -0.276 0.171
6			0° 45° 90°			
7	10	10	0° 45° 90°	26.07 20.00 10.33	.529 0.718 1.03	-0.379 -0.436 -0.068
8			0° 45° 90°			
9	10	10	0° 45° 90°	27.83 18.53 10.03	.5088 0.755 1.048	-0.4159 -0.400 -0.0513

factors is essential, it is impossible to analyze the accuracy of the method by comparing known and measured stresses. One may, however, calculate the orientation of the principal stresses from the hole drilling data alone. Using equation 9 one calculates $\theta = 45^0$, which is far from the true value $\theta = 0^0$. We must conclude then, that the method as presently implemented is not useful for accurate stress analysis.

In searching for an explanation for these poor results, one may question the suitability of the instruments. The extensometers gave stable and repeatable results in calibration tests. However, there is a possibility that they were too stiff for use with 3 inch gage lengths. Future tests should use softer extensometers, perhaps with semiconductor strain gages to increase their sensitivity. In addition, the gage points might be embedded more deeply in the ice to assure accurate measurement. The spread of the data for repeated, identical loads indicates that individual crystals in the gaged sections may trade off their loads in a variable fashion. However, the gaged sections did contain several crystals, which should have minimized this factor, and such a process would presumably take many minutes to occur. Further tests could use large holes to approach a more nearly continuum behavior. However, holes larger than 12 inch diameter are difficult to drill without a vehicle-mounted auger.

One possibility is that sea ice may behave as a highly non-linear material, even in its elastic range. Peyton's (1966) data supports this conclusion. Our tests with both internal and external pressure on an ice cylinder also support this possibility: based on linear elasticity, the response to internal pressure should have been about half the response to external pressure. Figure 11 shows a response significantly lower than this. If non-linear elasticity proves to be a major factor for sea ice, it is questionable whether stress relaxation techniques will be useful for *in situ* stress analysis.

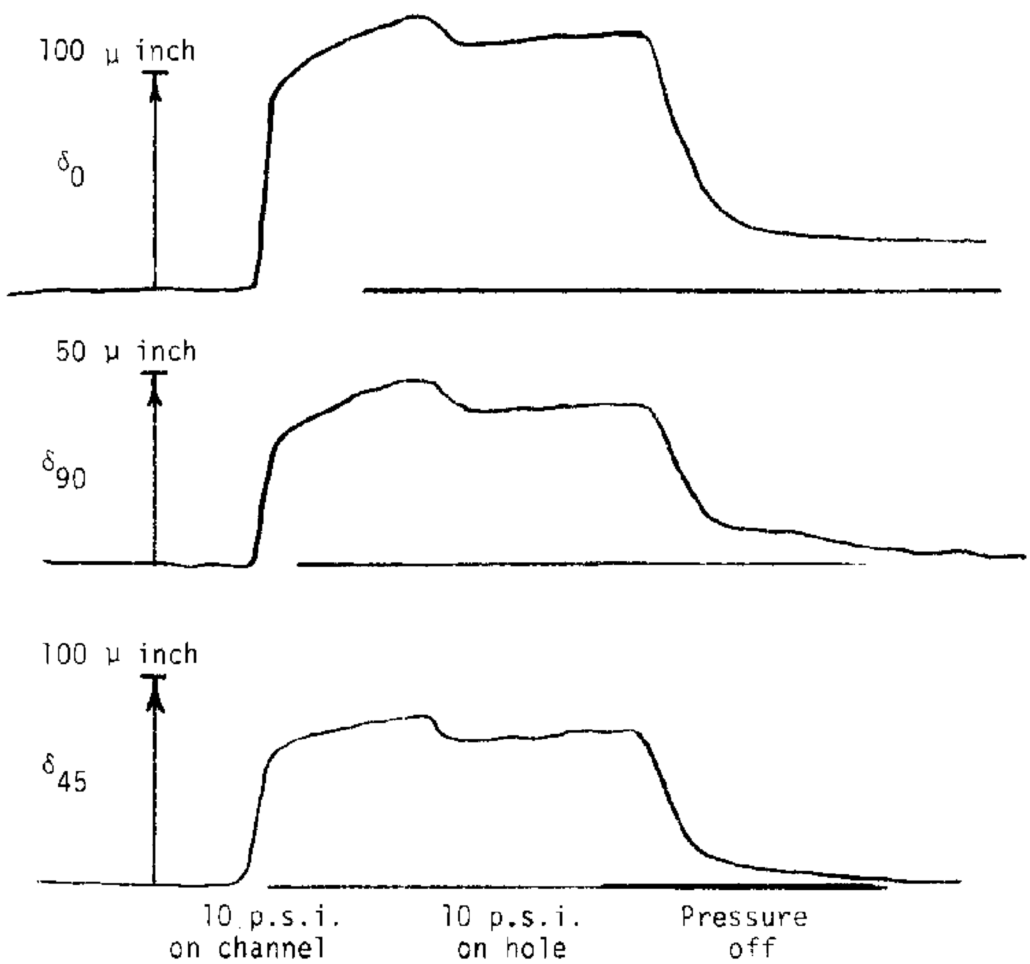

FIGURE 11. Strain transducer response to internal and external pressure on ice ring.

A final point is that the test described above took four hours to perform. In the field, a practiced team might be able to reduce this to two hours. At this rate, only three or four stress measurements could be made per day -- hardly enough to delineate an entire stress field.

IV. STRESS TRANSDUCER TECHNIQUE

A. Theory

The design of load cells to be used as stress transducers has been discussed in Section II. These designs were based on the requirement that the transducer be stiffer than the surrounding ice and the background for this criterion was discussed in Section I. Exact design according to this criterion would entail the solution of a difficult problem in solid mechanics for each new transducer. However, the following one dimensional approximation is a useful design guide. Once a specific design is selected, its stress sensitivity may be determined by full scale tests or by computer aided analysis.

Figure 12 shows a spring-dashpot analogy to the problem of an elastic transducer embedded in a visco-elastic medium. The transducer is shown as a spring of modulus K_T while the surrounding ice is shown as a set of springs and dashpots K_1, K_2, C_1, C_2 on the left and right of the transducer. We assume that both the transducer and the ice undergo the same deflection δ. The force, F, causing this deflection is divided between the transducer, F_T, and the ice. In this analogy the applied stress is F/3 if the transducer and each ice module occupy equal areas. The quantity read out is F_T, the "nominal measured stress" which will probably not be equal to F/3.

Consider a creep test in which a load F is suddenly applied to the relaxed array of springs and dashpots. The force in the transducer will assume some initial value and then increase as the dashpots creep. The

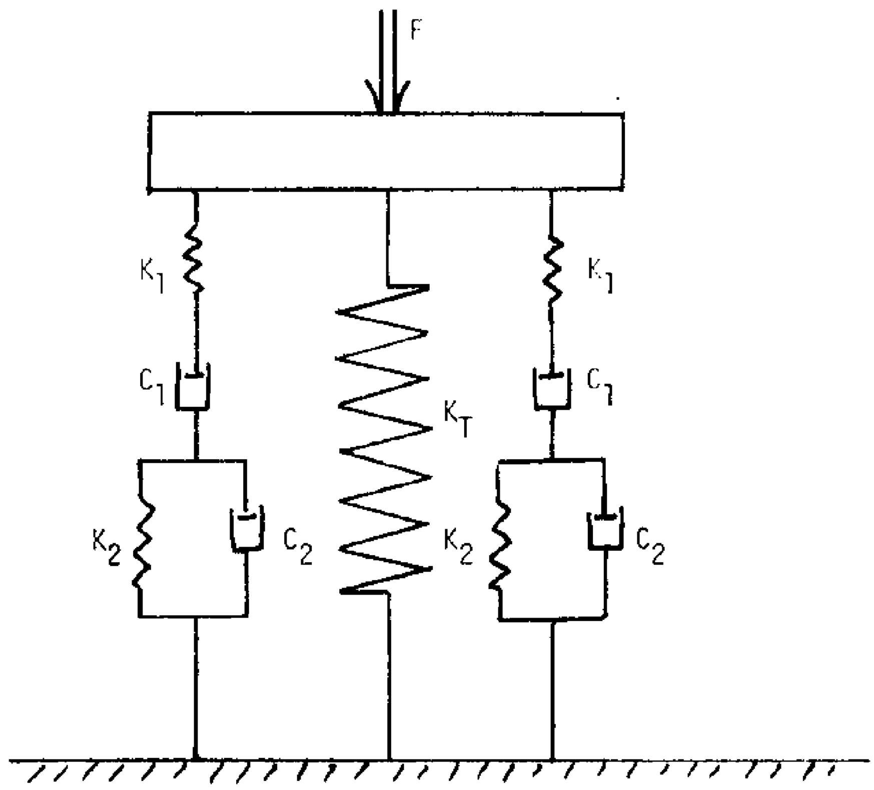

FIGURE 12. Spring-dashpot analogy to transducer/ice interaction.

The initial value can be found by assuming that all the dashpots are rigid.

$$F_T = F \frac{1}{1 + \frac{2K_1}{K_T}} \quad \text{Initial value} \tag{11}$$

If the dashposts are allowed to creep continuously, the transducer will eventually support the entire load:

$$F_T = F \quad \text{Final Value} \tag{12}$$

Notice that the final "nominal measured stress" is thus three times the "applied stress", i.e., there is a stress concentration factor of three.

The relation in equation 11 is plotted in Figure 13, with heavy arrows showing the direction in which the relation proceeds as creep occurs (essentially softening the ice). Figure 13 shows clearly why a soft transducer is not satisfactory for use in a creeping material. Even a transducer which identically matches the elastic modulus of the host ($K_T = K_1$) is unsatisfactory since the final value of the transducer reading is three times the initial value, even though the applied stress is constant. Choosing a transducer with $K_T/K_1 > 10$ minimizes the uncertainty due to creep to 16 percent. Choosing a stiff transducer also minimizes the problems of the uncertain and variable elastic behavior of sea ice if a maximum expected value of elastic modulus is used. Thus two basic and formidable problems are solved by the choice of a stiff stress transducer. In this model, the final stress concentration in creep is, of course, fixed by the choice of two ice modules adjacent to the transducer and by the rigid shear coupling between the ice and the transducer head. Because of these assumptions, the final value does not reflect the ratio of shear to compressional ice creep stiffness as found in Berry and Fairhurst's solution (1966) for the cylindrical stress gage. Indeed, that creep stiffness ratio probably determines the number of ice modules which must be associated with each transducer by governing the final stress concentration.

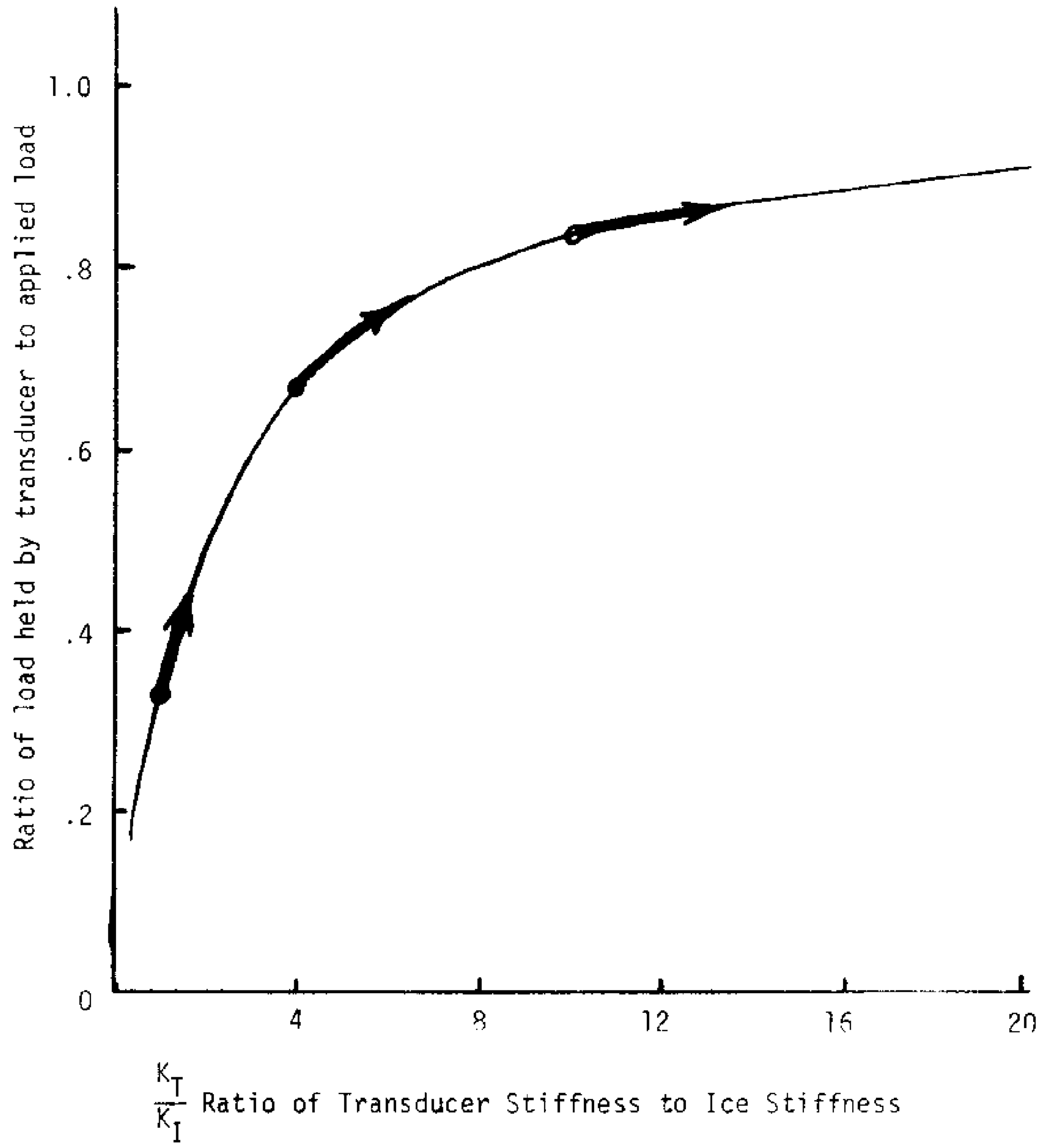

FIGURE 13. Percentage of applied load carried by transducer as a function of transducer to ice stiffness ratio, calculated from equation 11.

However, for any given number of adjacent modules, only a stiff transducer will enable the elastic response to be close to the creep response.

It is of interest to evaluate the response of this model to more complex variations of stress with time. For this purpose, we may write a transfer function relating the output F_T to the input F.

$$\frac{F_T}{F} = \frac{T_1T_2D^2 + [T^2+(1+\frac{K_1}{K_2})T_1]D+1}{(1 + \frac{2K_1}{K_T})T_1T_2D^2 + [(1+\frac{2K_1}{K_T} + \frac{K_1}{K_2})T_1+T_2]D + 1} \tag{13}$$

D = the differential operator, $\frac{d}{dt}$

with $T_1 = \frac{C_1}{K_1}$

$T_2 = \frac{C_2}{K_2}$

The usual Laplace Transform techniques can then be used to relate the transducer's response to a given input. Figure 14 shows the log-magnitude and phase versus frequency plots obtained from equation 13 for a sinusoidal input. The values for T_1 and T_2 were calculated from Tabata's work, quoted in Weeks and Assur (1969), which gives values for the rheological constants of sea ice used in this model as:

$K_1 = 1.1 \times 10^9$ dyne/cm^2

$C_1 = 1.2 \times 10^{11}$ dyne-min/cm^2

$K_2 = 1.8 \times 10^9$ dyne/cm^2

$C_2 = 2.7 \times 10^{10}$ dyne-min/cm^2

thus

$T_1 = 125$ min

$T_2 = 14$ min

Figure 14 also assumes $K_T = 10K_1$. Using these data, both the numerator and denominator of equation 13 are highly damped second order terms, implying that the response of the transducer in this model will show no resonant peaks. That is, there will not be the possibility of a buildup of un-relaxed stress in the host giving an excessive reading in the transducer, although there will be some phase and amplitude distortion of a complex stress wave.

The analysis given above forms a useful framework of expectations for stress measuring transducers. Naturally the details of ice/transducer behavior in the real world may be different in absolute magnitude, but we anticipate that if the transducer is sufficiently stiff the material properties of the ice will cause a minimum of uncertainity in the measured stress and both rapid and slow stress changes can be recorded and analyzed. The question of how stiff the transducer must be depends on how much of the surrounding ice is affected by its presence. Here we assumed that the affected area of ice was twice the projected area of the transducer and obtained a stress concentration factor of three. Actual tests described below give a stress concentration factor of four to five implying that the stress affected area is at least three times the projected area of the transducer.

B. Placement of Transducers

The stress transducers described in Section II were placed in artifically grown blocks of salt ice for use in evaluation tests. In each case the axis of the transducer was perpendicular to the growth direction of the ice. Two techniques were used for placement. For ice to be tested in the universal testing machine, a block approximately 8 inches x 8 inches x 12 inches was cut in half and a form-fitting hollow chiselled for the transducer. The two halves were then cemented together with a thin layer of fresh water. For tests in the large growing/testing tank, a block was quarried out to half the depth of the

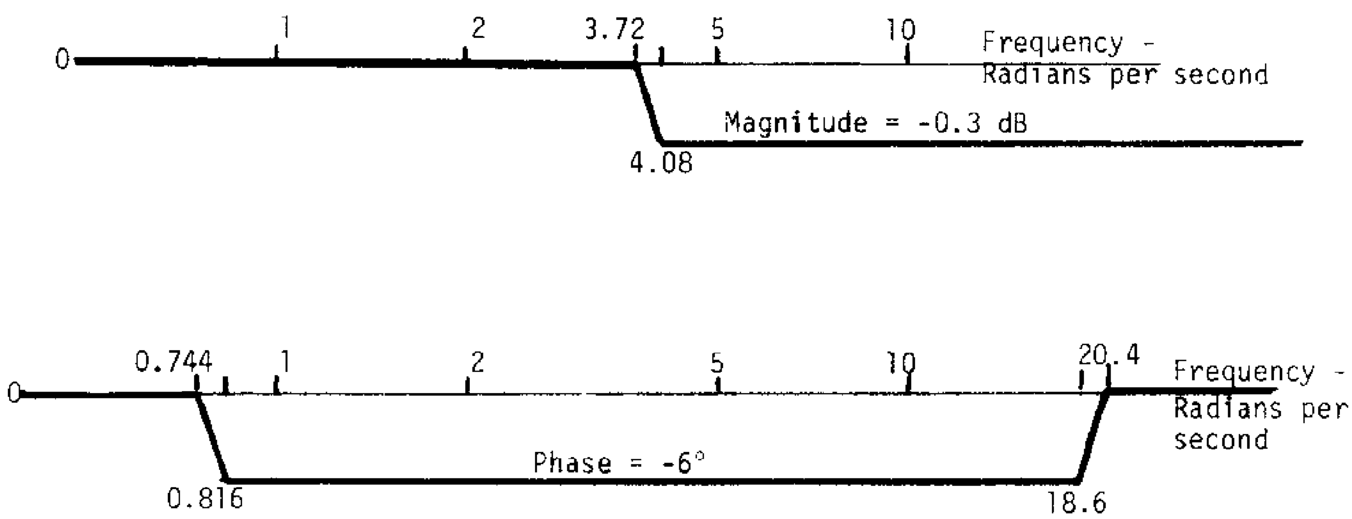

FIGURE 14. Log-magnitude and phase versus frequency plot for transducer/ice interaction from equation 13 using Tabata's rheological constants.

tank, a form fitting hole was cut or melted for the transducer, the block was replaced, and the trench was filled with fresh water. In each case brine accumulation in the transducer hollow was sponged dry just prior to adding the fresh water. In this way the possibility of brine accumulation at the transducer/ice interface was minimized. The transducer strain bridges were balanced prior to freeze-in so that a true zero load reading could be established.

C. Experimental Data

Figures 15 through 17 show the behavior of three transducers in a 32 x 38 x 12 inch deep block of ice under uniaxial compression. In each case, the transducer output is shown as the "nominal measured stress" which is taken as the force sensed by the transducer divided by the projected area of the transducer head, $\pi/4$ square inches. This is not expected to be equal to the applied stress. The transducers were buried 6 inches deep with their stress measuring axes at 0^o, 45^o, and 90^o to the stress direction respectively. In this way, the behavior under direct compression, shear plus biaxial compression, and transverse compression could be evaluated. Three types of data were gathered: response during creep at 10 psi compression, response to a "square wave" consisting of 10 psi compressive pulses, and response to loads high enough to cause ice failure. The creep test was carried on for 10 days then the block was allowed to sit for another 20 days under zero load. During the entire 30 days, periodic square wave loading tests were performed, and the ambient temperature was varied between -1^oC and -22^oC. The ice containing the 0^o and 90^o transducers was then cut out as an 8-1/2 x 7-5/8 x 15 inch high block. The 45^o transducer was cut out as a separate block. Both blocks were then temperature cycled for 24 and 48 hours from -8^oC to -22^oC. Finally, the

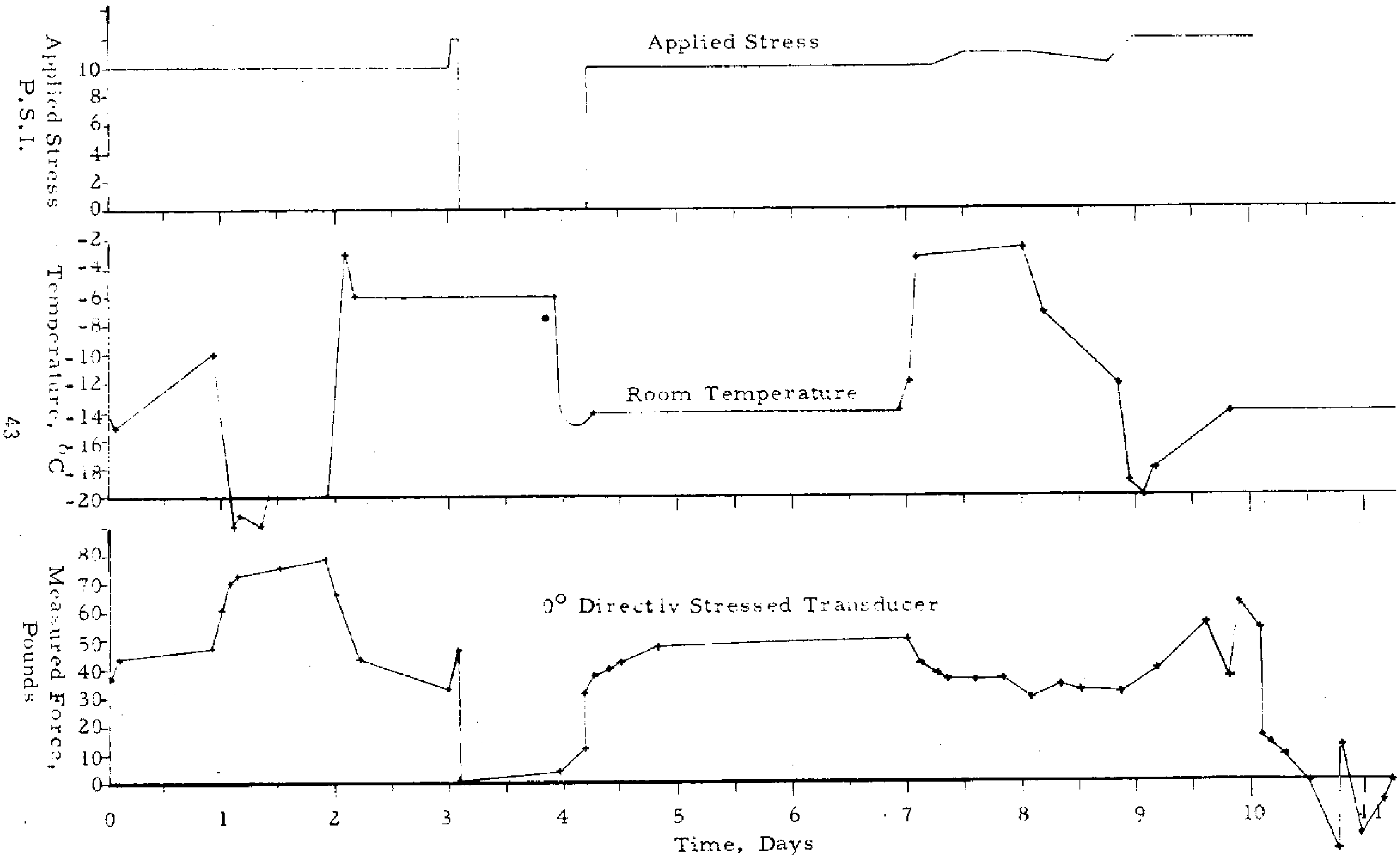

FIGURE 15a Applied stress, room temperature, and 0° stress transducer output during creep test, #6.

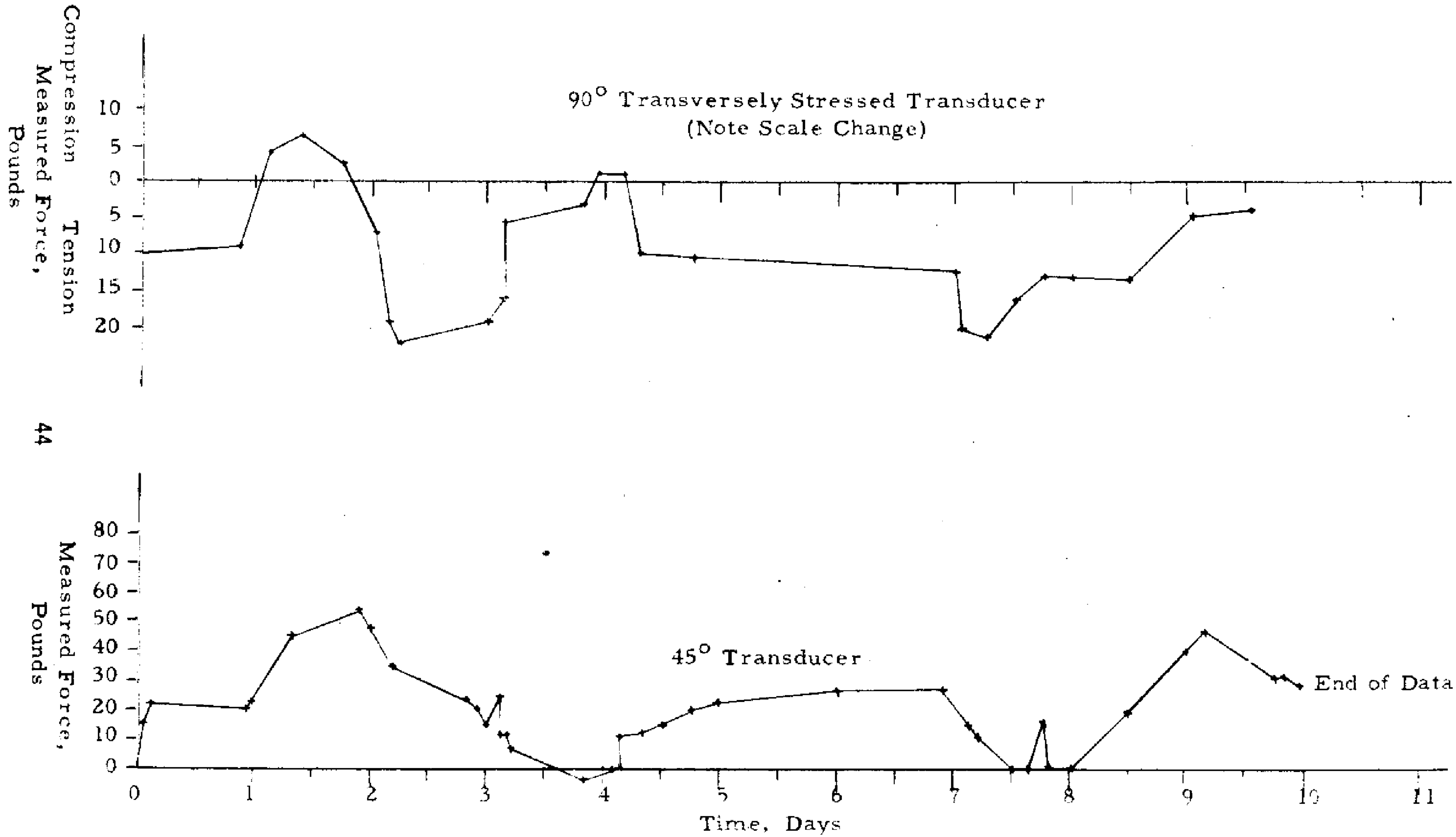

FIGURE 15b 90° and 45° stress transducer outputs during creep test, #6.

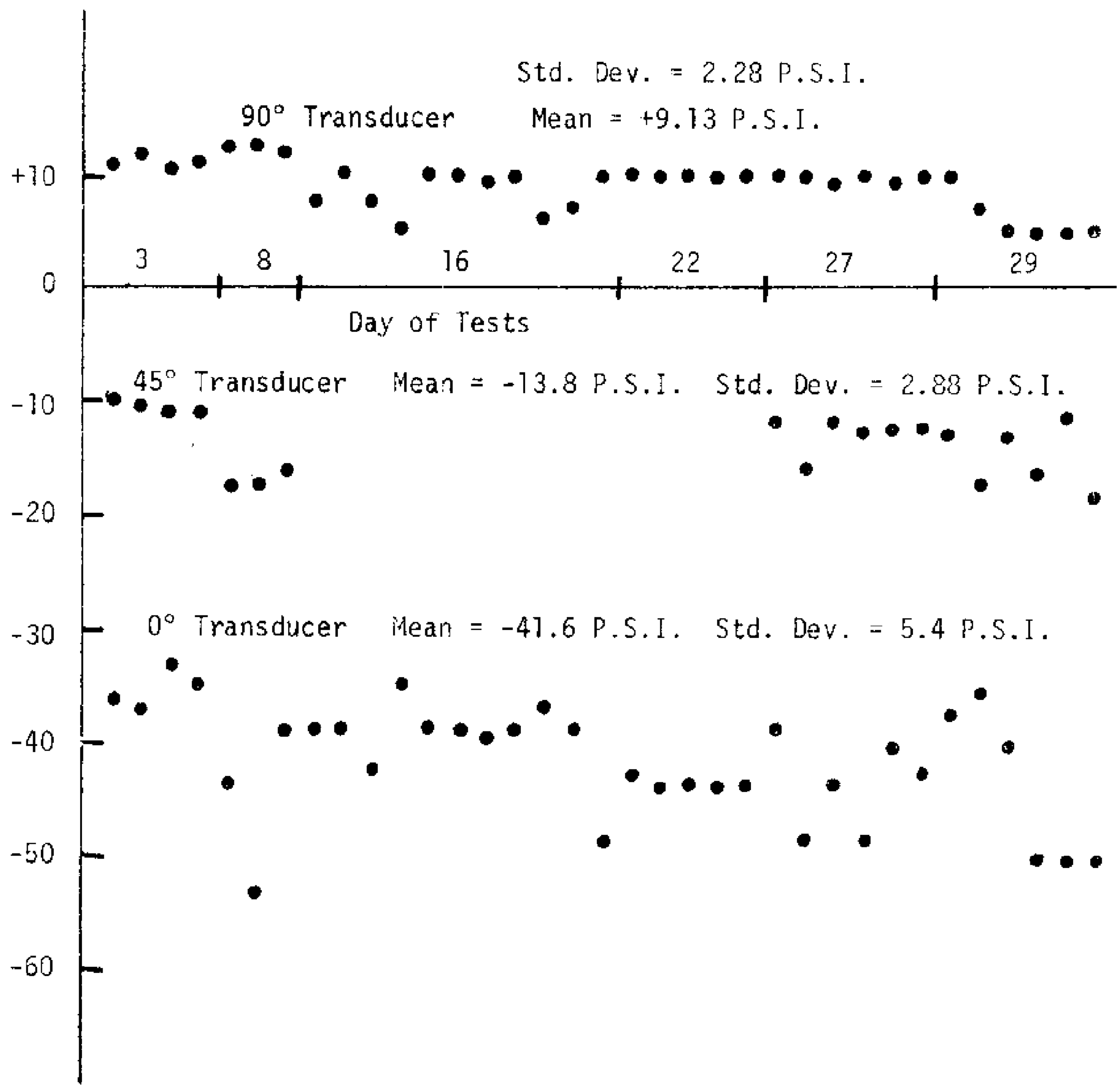

FIGURE 16. Response of transducers in Figure 15 to rapidly applied loads.

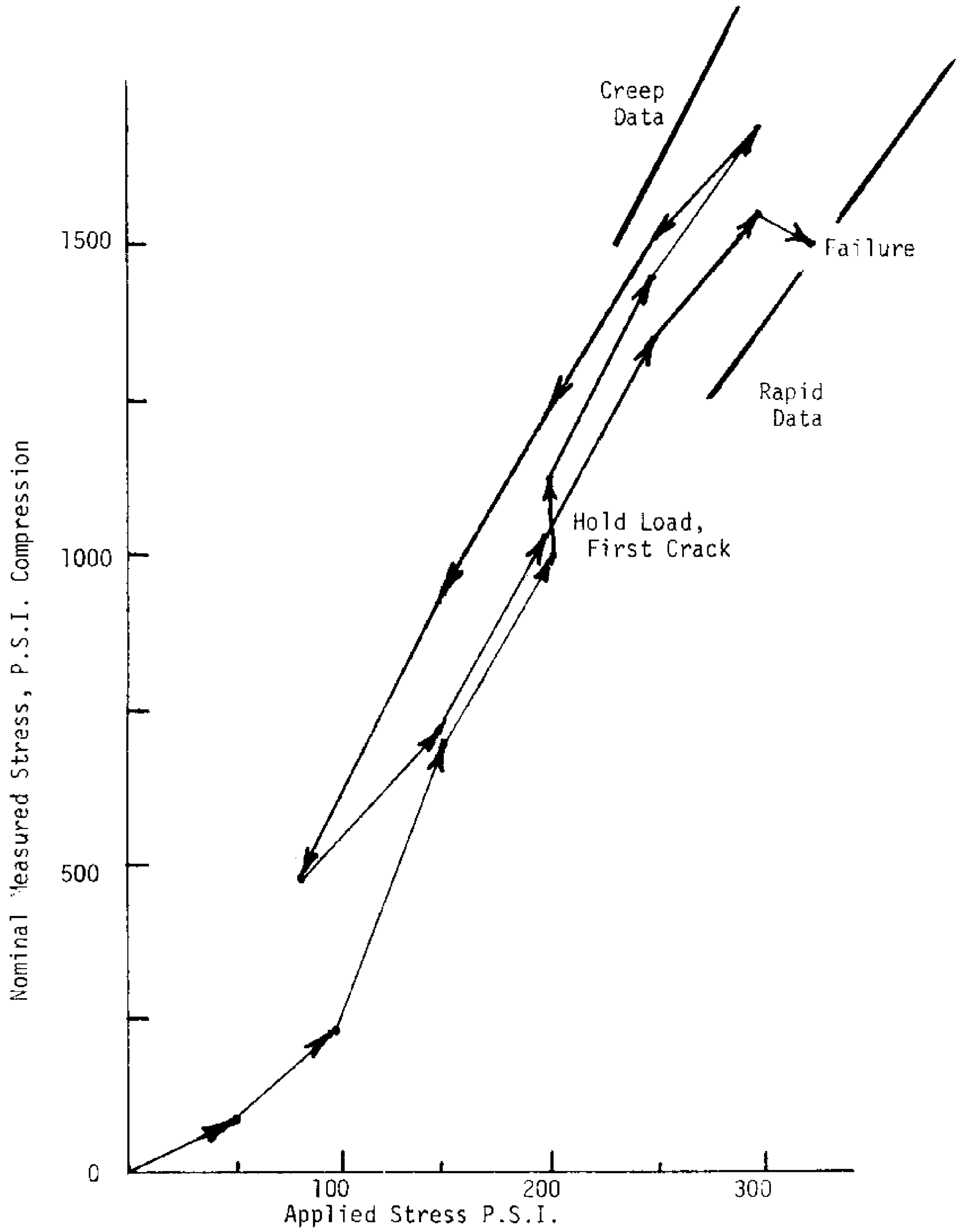

FIGURE 17a Response of transducer to direct compressive stress causing ice failure. Transducer was formerly at 90° to stress in Figure 16 and 17.

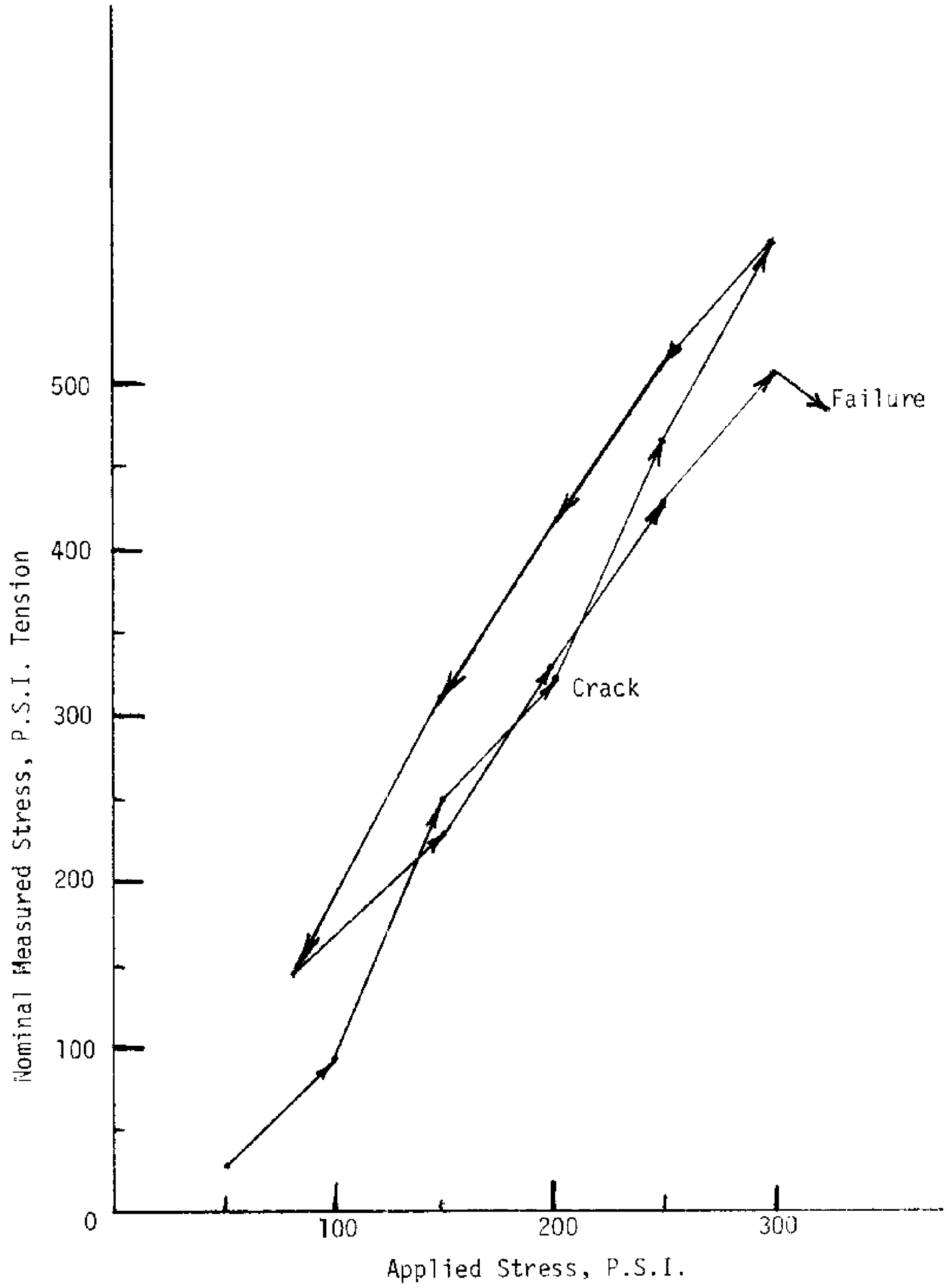

FIGURE 17b. Response of transducer to transverse compressive stress causing ice failure. Transducer was formerly at 0° to stress in Figure 16 and 17.

block containing the 0^0 and 90^0 transducer was loaded to compressive failure in the 30,000 lb. testing machine. In doing so, the stress direction was changed 90^0 so that the 0^0 transducer was loaded transverse to the compressive axis while the 90^0 transducer recorded direct compressive failure. The failure test consisted of loading until cracking could be heard or seen, unloading, and loading again until failure was well progressed. The first loading was at about 100 psi per minute, the second loading was at about 200 psi per minute. The ice temperature was about -10^0C.

Table 3 summarizes the data given in Figures 15, 16, and 17 and presents data from several other tests. In each case, the data is given as a stress concentration factor which is calculated as the ratio of "nominal measured stress" to actual applied stress. Test 3 is the only tension test performed. Due to the difficulty of gripping and uniformly loading ice in tension, Test 3 was performed as a thick tube with internal pressure. A tube 16 inch inside diameter by 30 inch outside diameter by 12 inch axial length was loaded under 10 psi internal pressure using an air bag. This placed the tube under radial compression and tangential tension (hoop stress) which was sensed by a tangential stress transducer at an 11.5 inch radius. The resulting data was corrected for biaxial stress as described later. The applied stress was calculated using elastic theory for thick cylinders. A 5 x 5-1/2 x 10 inch high block containing the transducer was then cut and tested in compression to failure.

Figure 18 shows a typical transient response obtained as a transducer is being frozen into an ice block.

Figure 19 shows the results of a temperature sensitivity test in which a block of ice containing a transducer was cooled by rapidly dropping the

TABLE 3a

DIRECT LOAD STRESS CONCENTRATION FACTORS.

All Stresses compressive, except as noted.

Test	Applied Stress	Stress Concentration Factors		
		Creep	Failure	Rapid Loads
1	80 psi	3.4		
	342 psi		3.6	
2	84 psi			3.92
3	10 psi, T	4.35		3.4
	1000 psi		4.1	
6	10 psi	6.4		4.16
	334 psi		5 to 5.41	

TABLE 3b

TRANSVERSE LOAD STRESS CONCENTRATION FACTORS.

All applied stress compressive.

Test	Applied Stress	Transverse Stress Concentration	Transverse Stress Concentration / Direct Stress Concentration
1	Creep 80 psi dropping to 40 psi	$-0.82 \rightarrow -0.082$	$-0.24 \rightarrow -0.02$
6	Creep, 10 psi	-1.53	-0.24
	Rapid, 10 psi	-0.91	-0.28
	Failure, 334 psi	-1.5	$-0.278 \rightarrow -0.3$

FIGURE 18. Freeze-in transient stress.

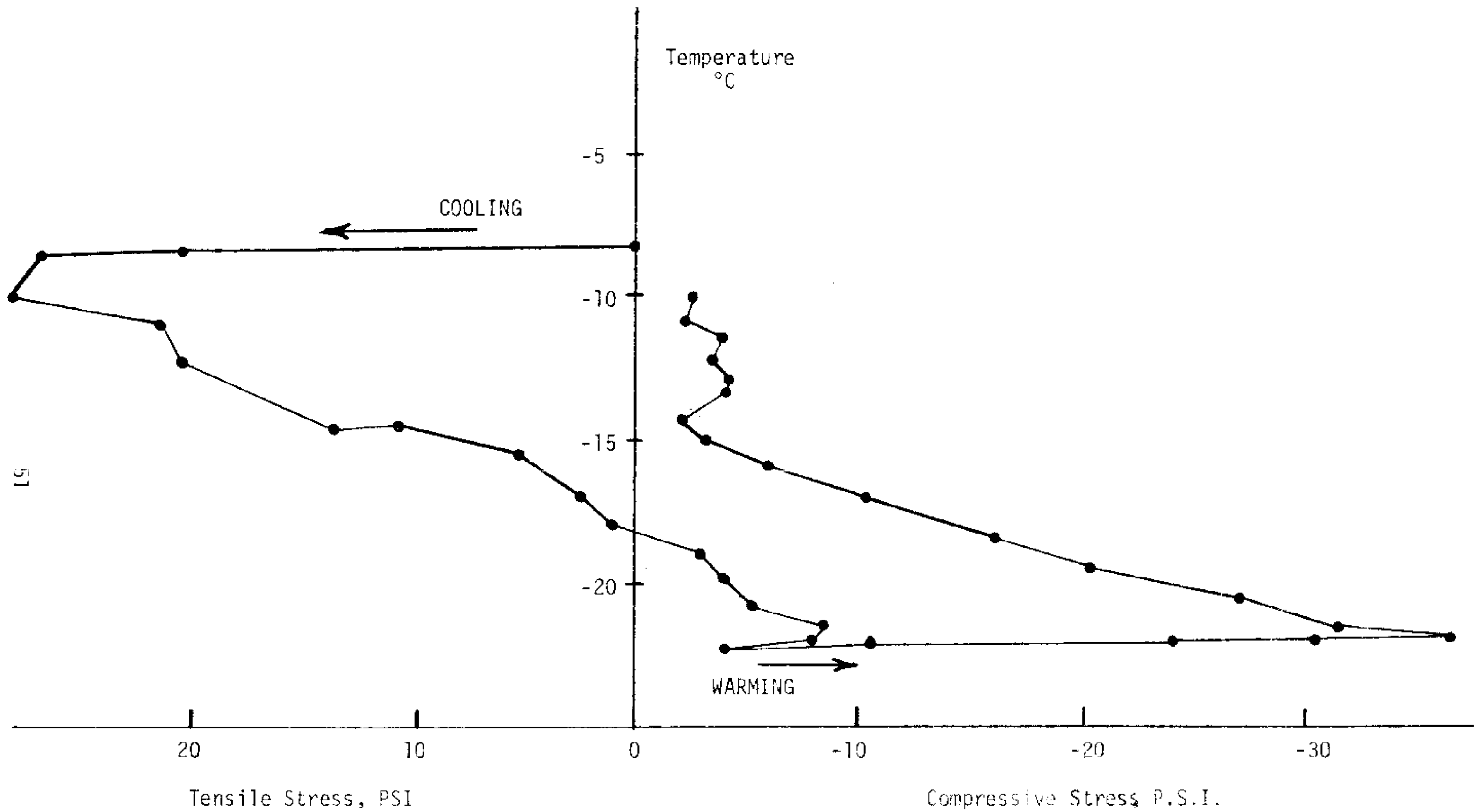

FIGURE 19. Temperature sensitivity of transducer in ice block.

room temperature. The data has been corrected for zero shifts due solely to the temperature of the transducer or due to the temperature of the electronic instruments.

One factor should be mentioned concerning creep Test 6. A significant zero drift occurred between the time the transducer was placed in the ice and after it was removed: nearly 100 pounds for the 0° transducer. This has been apportioned to the data and substracted for Figure 15. Some corrosion was noticed on the transducers and it is possible that very small amounts of brine could have penetrated to the strain gages, shifting the overall balance of the strain bridges. Another possibility is that the solder used on the strain gages was subject to "tin disease", a low temperature phase transformation of tin which can occur in 63% tin-37% solders below 20°F. Such a change could alter overall bridge balance also.

D. Discussion

In discussing the suitability of load cells for stress measurement, it will be convenient to consider first only the data for transducers whose axes are parallel to the applied stress. The fact that all data show a significant stress concentration should not be surprising, as it is consistent with the spring-dashpot model discussed previously. The transducer, being stiffer than the ice, simply supports more than its share of the load. The exact value of the stress concentration is, of course, dependent upon transducer geometry and the degree of adfreeze bonding in areas of the ice-transducer interface which are under tension. The transducers used here were coated with silicone rubber, and little adfreeze strength was expected. A stress concentration factor of four to six is probably typical of long, thin geometries, as used here. A small amount of data gathered with a 3 inch diameter by 1 inch long transducer indicated reduced stress concentration factors for short, squat geometries.

Figure 15 shows that the response of a directly stressed transducer to creep loads is acceptably constant. For 10 psi constant applied stress and nearly constant room temperature, the stress in the transducer reached a steady value in six hours, and this sensitivity was maintained for the full 10 days of the test. In another test, Test 1, loaded at 80 psi, measurements indicated that the stress concentration in the transducer reached a steady value within one hour which was maintained +15% for the entire six days of the test, during which time 1/2% axial strain was measured for the block.

One point that should be made in considering the data in Figure 15 is that a definite temperature effect is evident. Since the data has been corrected for both electronic and transducer temperature sensitivity, the remaining variation in measured stress must be interpreted as being thermally induced stress actually present in the ice. The trends in the data are consistent with this interpretation. For instance, the increase in compression registered about 20 hours after the start of the test could be caused by the top surface of the ice going into tension as the room cooled to -20°C (the ice was in the insulated testing tank with only its top surface exposed). There was a lag of several days between room temperature and ice temperature at the transducers so that the almost daily cycling of temperature could have been produced by very complicated thermal stress profiles.

To further investigate temperature sensitivity, ice blocks containing the transducers from the creep test were temperature cycled fully exposed to cold room air. Figure 19 shows a typical set of data for a 48 hour test, corrected for electronic and transducer temperature sensitivity. Data points are taken at 1 hour invervals. It is likely that this block was of low enough salinity that it had a non-linear positive coefficient of thermal expansion (expansion with increasing temperature) (Malmgren, 1927). Rapidly cooling the room then induced contraction of the outer layer of ice, probably resulting in a triaxial stress field around the transducer. Presumably the stresses transverse to the transducer's axis provided the dominant signal, resulting in the apparent tensile stress. The reverse occurred on warming the room. The fact that the transverse stresses dominated is unusual and could perhaps be due to the size or shape of the block. It is not known whether similar behavior could be expected for a large block. It is significant that as soon as thermal equilbrium was attained in the ice block, the transducer reading approached and remained near zero stress.

The transducers were designed assuming a stress concentration of 2.0 and ice whose elastic modulus was 10^6 psi. The initial response was 70% of the final creep response, indicating that the elastic modulus of the ice may have been lower than 10^6 psi. We conclude that stiff transducers can indeed measure stress while creep occurs.

Figure 16 shows the response of the transducers to "rapid" square wave loading. Several tests of 1, 2, 5, and 10 minutes duration were performed on each of five days. Asympototic approximations similar to those described in the hole drilling analysis were used to reduce the data, and no specific difference was noticed between 1 minute and 10 minute tests. In general, tests with the load going from 10 psi to zero gave slightly more response than tests from zero to 10 psi. The average for the direct loaded transducer is 41.6 psi with a standard deviation of 5.4 psi. The experimental accuracy for setting the load was +5% and the accuracy for reading the charts was +2 pounds. The data seem to indicate a slight increase in both sensitivity and spread as time progressed. It is possible that the method of data reduction induces an unnecessary spread in results. This would be particularly true for the data of day 21 and day 25, since a leak in the loading system made it difficult to apply the stress rapidly. Basically, however, the response is uniform.

The ability of the transducers to follow failure of the surrounding ice is shown in Figure 17a. The hysteresis in Figure 17a gives evidence of creep and relaxation of the ice surrounding the transducer. Even after the first cracks appeared in the ice, the transducer followed the increasing stress quite well. At the second, more rapid loading, the transducer again followed the applied stress until there was extensive cracking and gross failure destroyed the continuum nature of the block. It is interesting to note that the failure data lies between the best fit calibrations (stress concentration factors) for creep and for rapid loads. Apparently either type of test provides a good approximation to the failure calibration of the transducers. This is important for field use of transducers because large scale failure tests of ice _in situ_ are costly while _in situ_ creep and rapid responses can be found using air bag techniques. On the other hand, laboratory calibrations are expediently done as failure tests.

Most of the ice tested here failed at about 300 psi although one block withstood 1,000 psi, Test 5. Apparently the details of its growth, crystallography, and aging resulted in an ice quite different from the others tested. It is important that the transducer response for this unusual ice did not differ greatly from the other failure tests, as shown in Table 3.

The only available data for the response of transducers to tension is from the hoop tension test, Test 3. The stress concentration factor in tension is seen to be consistent with the data for this block and for other ice blocks in compression. Tensile failure tests could not be done with our equipment. However, the large tensile loads indicated by transducers oriented perpendicular to the stress direction in failing ice blocks imply that tensile failure could have been followed without destroying the ice-transducer bond. It is not known whether stress concentration in the ice near a transducer would initiate premature tensile failure.

Figure 18 shows the transient response as a transducer is frozen into an ice sheet. Compressive stress is induced as the fresh water around the transducer freezes. This stress relaxes within several hours, or if the ice is already stressed, the transducer reading approaches that stress. Except for very cold ice under low stress, it is likely that 24 hours would be more than sufficient time for the transducer to attain a true reading.

Since these transducers are to be used in field experiments, it is likely that there will be no control on the type of ice in which they are placed. This makes it important to discuss the uniformity of their response, summarized in Table 3. For any given type of test -- rapid, failure, or creep -- there is a variation in the calibration constants or stress concentration factors obtained. Indeed, even for repeated rapid tests of the same ice/transducer combination there is a spread which cannot be entirely attributed to experimental error. Some of this variation could be due to the crystallography of the sea ice matrix. It is likely that specimens three and six had more uniform, finer grain structure than specimens one and two since greater control was exercised in growing them. Thus, Tests 3 and 6 may be more representative of "continuum" behavior when the grain size is small in relation to the transducer. It is important that the consistency is much better for a given specimen of ice. For instance, the failure data in Test 6 was taken with the 90° transducer while the creep and rapid data used the adjacent 0° transducer, but the results fit together well. Not enough data has been gathered here to allow a complete statistical analysis of expected accuracy. However, it is clear that rigid stress transducers can provide useful stress information, and the data of Table 3 indicates that use of an average stress concentration factor will enable stresses to be measured within +22 percent of the true value. Quite probably, much more accuracy can be obtained with further development of the technique. For example, the use of much larger transducers is highly recommended. Confidence in the calibration constant (stress concentration factor) will be greatly improved if in situ calibration can be done, and this is easily accomplished using air bag techniques. For instance, a rectangular block containing the embedded transducer can be quarried free and tested in place with a flat jack on one face. Either direct or transverse sensitivity can be obtained. Another possibility is to drill a vertical hole near a transducer and use an air bag to give internal pressure. If an ice ring were cut, tensile calibration could be performed. In any event, both rapid and creep calibrations should be obtained so that the investigator may choose which is applicable to his case.

E. Discussion of Biaxial Loading

The data in Figures 15, 16, and 17 indicate that stresses perpendicular to the stress measuring axis of a transducer also produce a response. This transverse sensitivity is opposite in sign to the stress causing it; i.e., a compressive stress results in a tensile signal from a transverse sensor. Table 3 presents the data for several tests in the form of the transverse stress concentration factor which is taken as the ratio of the nominal measured stress to the transversely applied stress. Also tabulated are the ratios of transverse stress concentration to direct stress concentration for the same or nearly identical blocks of ice. It was felt that the length to diameter ratio of a transducer might be important in determining the magnitude of the transverse response. However, the transverse to direct response ratio for transducers with $\frac{L}{D} = \frac{3}{1}$ was found to be similar to that of transducers with $\frac{L}{D} = \frac{1}{3}$.

Consideration of the Poisson ratio effect makes it easy to see why a traverse response should occur: a block in compression will try to expand laterally and this will in turn stretch the transducer. With ice, plastic flow occurs at nearly any stress level, and this increases the problem by continually feeding a flow of material around the transducers. The traverse reading at any time depends upon a balance of this flow against the load in the transducer. Thus we find that the ratio of transverse to direct response is nearly the same for rapid low level and rapid failure tests both of which have high strain rates. For the low strain rates of a creep test, the stress concentration may continually relieve itself and Table 3 shows that the transverse to direct response dropped nearly to zero because the load was allowed to drop slowly to about half of its original value over 24 hours (Test 1).

In the usual case, stress transducers will be used to measure stress in a multi-axial stress field and we must therefore discuss the ability of these transducers to measure a stress tensor. For the case of a floating or land fast sheet of sea ice, the significant stresses will be in the plane of the ice sheet, although bending may introduce small out-of-plane stress components. Thus we may confine ourselves to the question of measuring the components of the stress tensor in plane stress. Since the principal stress directions will be unknown, we must determine three quantities: the principal stresses σ_1 and σ_2 and their orientation θ relative to some reference axes. This requires three independent measurements of stress and is often accomplished by the use of three gages (measuring stress or strain) in a 0^o -45^o -90^o array or rosette as shown in Figure 20. If a gage, say gage 0, is sensitive to <u>only</u> stress along its axis then the <u>measured stress</u> σ_{0m}, σ_{45m}, σ_{90m} will also be real stresses σ_0, σ_{45}, σ_{90} in the 0^o, 45^o, 90^o directions and may be used directly to compute the principal stresses and their orientation. Mohr's circle provides an easy way of handling this. The transducers developed here have a significant transverse sensitivity so that the measured stresses are only apparent stresses. That is,

$$\sigma_{0m} = \alpha\sigma_0 + \beta\sigma_{90} \tag{14}$$

$$\sigma_{90m} = \beta\sigma_0 + \alpha\sigma_{90} \tag{15}$$

with

σ_i = actual stress for orientation i

σ_{im} = stress measurement for orientation i

α = direct stress concentration factor

β = transverse stress concentration factor

it can be shown that the measured stress in the 0 direction is related to the true principal stresses by

$$\sigma_{0m} = (\alpha+\beta)\,\frac{\sigma_1+\sigma_2}{2} + (\alpha-\beta)\,\frac{\sigma_1-\sigma_2}{2}\cos 2\theta \tag{16}$$

It follows from this that a Mohr's circle may also be constructed for the measured stresses which will yield measured or apparent principal stresses σ_{1m}, σ_{2m}. These measured principal stresses have the same direction as the real principal stresses. The real principal stresses may be obtained by inverting equations 15 and 16.

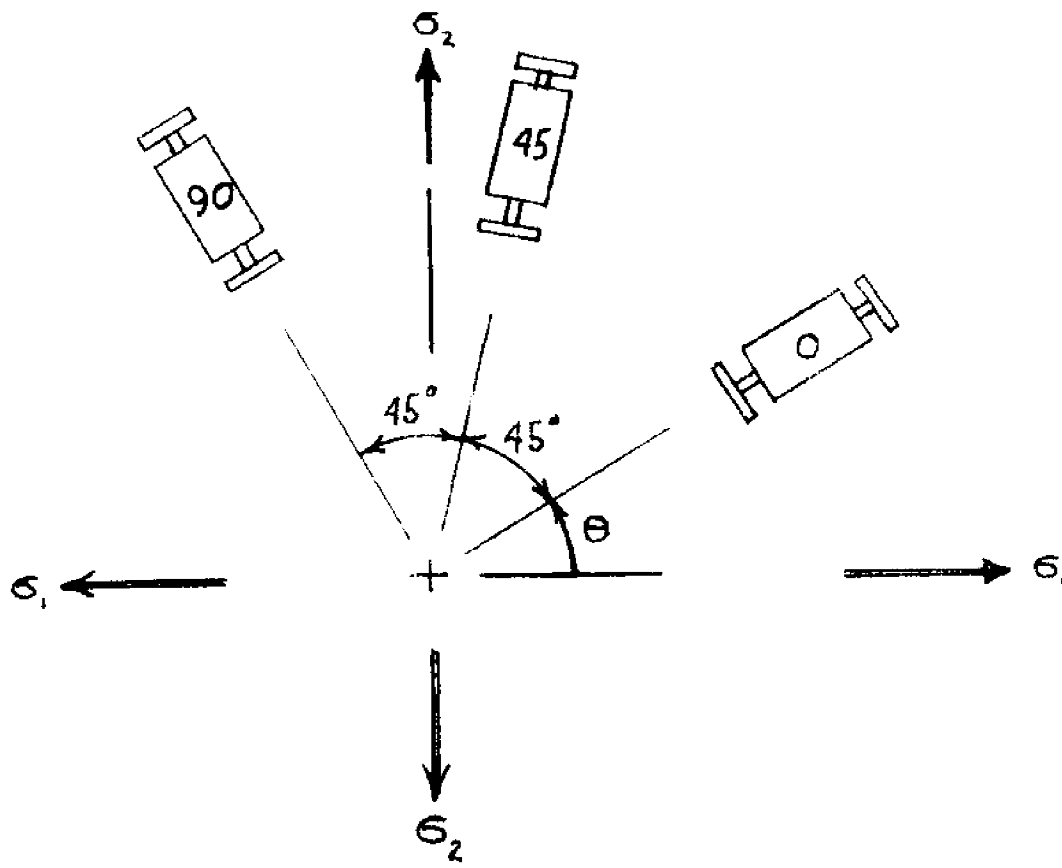

FIGURE 20 Rosette of stress measuring sensors.

$$\sigma_1 = \frac{\alpha}{\alpha^2 - \beta^2} \sigma_{1m} + \frac{\beta}{\alpha^2 - \beta^2} \sigma_{2m}$$

$$\sigma_2 = \frac{\beta}{\alpha^2 - \beta^2} \sigma_{1m} + \frac{\alpha}{\alpha^2 - \beta^2} \sigma_{2m} \tag{17}$$

An equivalent situation exists when stress fields are calculated from strain fields where the transverse sensitivity appears as Poisson's ratio.

The data of Test 6 allows us to evaluate the accuracy of this analysis. For instance, after 20 hours, the direct transducer read -48 pounds, the 45^0 transducer read -18.5 pounds, and the transverse reading was +8 pounds. Use of Mohr's circle calculated from the 0^0 and 90^0 data predicts the 45^0 transducer should read -16 pounds. This is a 15 percent error. A larger error is indicated on Day 6 after both temperature and stress equilibrium had been established. The 45^0 transducer reads 27 pounds, rather than 19 pounds as predicted by Mohr's Circle. It is possible that a relief of the transverse stress occurred for the 45^0 transducer due to the low stress levels. If complete relaxation occurred, the calculated value would be 25 pounds which is close to the actual value.

The fact that the transverse sensitivity term can be significant means one must choose whether the sensitivity ratio for creep or ridge stress is more applicable. In some cases the choice will be clear; in other cases it will be necessary to calculate upper and lower bounds, perhaps even assuming the transverse response to be zero. Certainly investigations attempting to determine design limits on ice stresses will wish to do this and make the conservative choice.

We have shown here that stiff transducers can be used as stress sensors, while soft transducers will remain essentially displacement sensors. The transducers used by Tabata and Ono, Frederking, and Richardson have been described in the introduction, and there is no reason why they should not act as stress sensors provided they are sufficiently stiff and are capable of supporting tensile stress fields. In this respect, the use of lucite bars is not recommended since plastics have low elastic moduli. The use of an embedded ring or cylinder will be most successful only if great adfreeze strength can be realized. The selection of commercially available load cells must be preceded by an evaluation of their stiffness.

V. CONCLUSIONS

1) Embedded load cells can be used as stress sensors for sea ice in compressive creep, compressive failure, and moderate tensile stress situations.

2) In order to act as a stress sensor, a load cell must be stiffer than the surrounding ice.

3) Either creep or failure tests can be used to yield a useful sensitivity factor for a given transducer design.

4) Uniaxial stress sensors are also sensitive to transverse stress when embedded in sea ice.

5) Transverse sensitivity factors should be obtained for both creep loads and rapid loads (either short term low loads or failure loads).

6) An array of three stress sensors can be used to measure biaxial stresses, provided both direct and transverse sensitivity factors are known.

7) Transducers can be calibrated *in situ* using inflatable air bags.

8) More work must be done to develop a useful stress relief technique.

REFERENCES

1. Berry, D. C. and Fairhurst, C. 1966. "Influence of Rock Anisotropy and Time-Dependence Deformation on the Stress Relief and High Modulus Inclusion Techniques of Insitu Stress Determination", A.S.T.M. S.T.P. 42, 1966.

2. Dykins, J.E. 1966. "Ice Engineering - Tensile and Bending Properties of Sea Ice Grown in a Confined System:, U.S. Naval Civil Engineering Lab. Rept. R415 Y-F015-11-01-052.

3. Frederking, R. 1972. N.R.C. Canada, Ottawa, Canada, Personal communication.

4. Hawkes, J. 1969. "Stress Evaluation in Low Modulus and Visco-elastic Glass Inclusions", Experimental Mechanics, February 1969.

5. Hetenyi, M. 1950. Handbood of Experimental Stress Analysis, Wiley & Sons, New York.

6. Jaeger, J. C., and Cook, N.G. 1969. Fundamentals of Rock Mechanics, Methuen Co., Ltd., London, 1969.

7. Malmgren, F. 1927. In Scientific Results of the Maud Expedition, 1918-25.

8. Mather, J. 1934. "Determination of Internal Stresses by Measuring Deformations around Drilled Holes", Trans. Americ. Soc. Mech. Engineers, V86, 1934.

9. Milbrandt, K. 1951. "Ring Hole Method Determination of Residual Stresses", Proc. Soc. Exp. Stress Analysis, V9, N1, 1951.

10. Muskhelishvili, N.I. 1953. Some Basic Problems of the Mathematical Theory of Elasticity, P. Noordhoff, Ltd., Groningen, Holland, 1953.

11. Peyton, H. 1966. "Sea Ice Strength", University of Alaska, Geophysical Institute, Report UAG R-182.

12. Richardson, C. 1972. Arctic Submarine Laboratory, Naval Undersea Research Center, San Diego, California, Personal communication.

13. Riparbelli, C. 1950. "A Method for Determination of Initial Stresses", Proc. Soc. Exp. Stress Analysis, V8, N1, 1950.

14. Sackinger, W. 1972. Department of Electrical Engineering, University Personal communication.

15. San Miguel, A. and Duran, E. 1970. "On the Measurement of Stress in Solid Propellant", Experimental Stress Analysis, December 1970.

16. Sokolnikoff, I.S. 1956. Mathematical Theory of Elasticity, McGraw-Hill, New York.

17. Springer, R. 1972. "Continuous Observations of the Structural Changes in Deforming Polycrystalline Ice", Dept. of Atmospheric Sciences, University of Washington, Seattle, Washington.

18. Tabata, T. 1972. University of Hokkaido, Japan, Personal communication.

19. Timoshenko, S. 1956. Strength of Materials, Pt. II, Van Nostrand, Princeton.

20. Weeks, W. and Assur, A. 1968. "The Mechanical Properties of Sea Ice", Proc. of Cons. on Ice Pressures Against Structures, NRC Tech. Memo. 92, Ottawa, Canada.